CHEMICAL ENGINEERING SCIENCE
GENIE CHIMIQUE

VOL. I SEPTEMBER 1952 NO. 5

The mechanism of liquid-liquid extraction across stationary and moving interfaces

Part I. Mass transfer into single dispersed drops

J. M. COULSON and S. J. SKINNER*

The Imperial College of Science & Technology, London

(Received 24 March 1952)

Summary—Experimental data are given for the transfer of material by diffusion from a continuous phase to dispersed drops. The data are given for three conditions: (a) during formation of the drop, (b) for transfer to the drops rising through still liquor, and (c) for the transfer to the drops rising counter to the downflow of the continuous phase. The transfer effected during formation is almost independent of the time of formation of the drop. The overall transfer coefficient K (based on the average area of interface during formation) decreases with increasing time of formation of the drop but is practically independent of the size of the drop. Smaller drops attain more nearly to equilibrium with the liquor because of the increased area per unit volume.

The value of K during the rise of the drops increases with drop size and is directly influenced by the relative velocity of the drops and the continuous phase. Comparison of the results with those anticipated, assuming that the drops rise as spheres or that they renew their interface each time they rise through one diameter, suggests that the real conditions lie between these extremes. The time of exposure of the interface is a main feature in determining the actual value of K. The results are applied to the case of a perforated plate extraction column.

Résumé—Données expérimentales sur l'échange matériel par diffusion entre une phase liquide continue et des gouttes de liquide qui y sont dispersées. Ces résultats correspondent à trois cas distincts:

a) Formation de la goutte,

b) ascension de la goutte dans le liquide immobile,

c) ascension de la goutte à contre-courant de la phase continue descendante.

a)—Durant la formation de la goutte, l'échange est à peu près indépendant de la durée de formation de la goutte. Le coefficient global de transfert K (basé sur la valeur moyenne de la surface de contact durant la formation) diminue avec une durée croissante de formation mais reste pratiquement indépendant de la taille de la goutte. L'équilibre avec la phase continue est atteint plus rapidement avec de petites gouttes à cause de l'accroissement de surface par unité de volume.

b)—La valeur de K croît avec la taille de la goutte.

c)—La valeur de K est en proportion directe de la vitesse relative des gouttes et de la phase continue.

Les résultats expérimentaux paraissent indiquer que l'échange intervient dans des conditions intermédiaires entre les deux extrêmes: ascension de la goutte conservant sa forme sphérique ou renouvellement complet de la surface de contact chaque fois que la hauteur d'ascension atteint un diamètre. C'est la durée de contact à la surface de séparation qui est le facteur déterminant pour la valeur actuelle de K. Les résultats sont appliqués à une colonne d'extraction à plateaux perforés.

INTRODUCTION AND SCOPE OF PAPER

There have been a number of papers describing the performance of small laboratory liquid-liquid extraction columns [1], [2], [3], [6], [8], [9], in which the general treatment has been to apply the two film theory of mass transfer by diffusion, and to express the transfer obtained in the form of a general rate equation such as:

$$N/t = k_a(C_a - C_{ai})S = k_b(C_{bi} - C_b)S. \qquad (1)$$

On the assumption that equilibrium conditions exist at the interface and where the equilibrium relation is a straight line this relation may be written,

$$N/t = K_a(C_a - C_a^*)S = K_b(C_b^* - C_b)S. \qquad (2)$$

Eq. (2) avoids the determination of the concentration at the interface by the use of overall transfer coefficients K, which are related to the film coefficients by the equation,

$$\frac{1}{K_a} = \frac{1}{k_a} + \frac{H}{k_b}, \qquad \frac{1}{K_b} = \frac{1}{k_b} + \frac{1}{H \cdot k_a}. \qquad (3)$$

For any apparatus such as a column eq. (2) is conveniently written in the form

$$N/t = K \cdot S \cdot \Delta C_m \qquad (4)$$

where ΔC_m is the log mean driving force at the inlet and exit of the unit. Since S is often very difficult to measure it is frequently replaced by the term $a \cdot V$, where a is the interfacial surface per

* Present address: Monsanto Chemicals, England.

unit volume of the column and V is the volume of the unit. This gives the general transfer equation as,

$$N/t = K \,.\, a \,.\, V \Delta C_m. \tag{5}$$

This equation is widely used to calculate values of Ka from experimental data but as both K and a are variables and a is very difficult to measure, the results are not easy to interpret.

The disadvantage of the above equation is that it assumes steady state conditions whereas in practice one liquid is usually dispersed within the other and the concentrations and rates of mass transfer may vary with time. The simplest case of unsteady state mass transfer is the absorption of a pure gas in a still liquid and this case was studied by HIGBIE [4]. When the gas and liquid are first brought into contact there is a very high rate of absorption which progressively decreases with time. Assuming the depth of liquid to be infinite and GRAHAMS law of diffusion to apply

$$\frac{\partial c}{\partial t} = D \frac{\partial^2 c}{\partial x^2}. \tag{6}$$

Integrating we obtain

$$f = 2(C_e - C_0)\sqrt{\frac{Dt_e}{\pi}}$$

where f = amount absorbed in time t and

$$k_L = 2\sqrt{\frac{D}{\pi t_e}}. \tag{7}$$

The above differential equation can also be solved for various simple geometric shapes and such solutions have been given by NEWMAN [12]. The equations are important since they show k to be a function of the time of contact or exposure of the interface. They may be applied to extraction if it is borne in mind that there are two films instead of one but the process is often complicated by turbulence.

There is some evidence in the literature to suggest that K varies with the time of exposure of the interface but no quantitative information, and the present work was undertaken in order to study the influence of this variable and to obtain a more complete knowledge of the mechanism of extraction. In the first paper the mechanism of mass transfer into drops is considered while the second is concerned with extraction between continuous liquid streams.

Part 1. Mass transfer into single dispersed drops

The general equation for counter current extraction columns does not take into account the fact that the extraction takes place in three distinct stages. The first stage occurs when the drops form, the second when they rise or fall through the continuous phase, and the third when they coalesce. This cycle may occur only once as in spray towers, or be repeated as in sieve plate towers. The present work was aimed at separating these stages and studying them individually, data for the first two stages being obtained by direct experiment, and that for the third stage by difference.

Very few papers have been published on the transfer to single drops and the results are not as yet conclusive. SHERWOOD [7], passed drops of benzene or methyl isobutyl ketone containing a small percentage of acetic acid as solute into a column of water and measured the change in concentration of the inlet and outlet streams. He expressed the overall transfer coefficient in the form of eq. (4), using the change in concentration multiplied by the flow rate for N, and the total surface of the drops in the column at any one time for S. He found that K increased with drop size, and with the time of formation of the drop. By plotting the ratio of the unextracted solute to the total solute it is possible to extract, against the column height he found that some 40% of the extraction measured occurred during the formation of the drops. WEST [11], using a similar system and apparatus, however, obtained results which differed very considerably from those of SHERWOOD. LICHT and CONWAY [5] allowed drops of water containing acetic acid to fall through a small column of isopropyl ether, methyl isobutyl ketone, or ethyl acetate. Using different heights of column they extrapolated back their data to show that 18–20% of the total extraction occurred during drop formation.

The present work has been arranged to study these features individually and is conveniently arranged in three series:

Series 1. Mass transfer into forming drops.
2. Mass transfer into drops rising in a still continuous phase.
3. Mass transfer into drops rising in a continuous phase moving against the drops.

Two systems have been used, benzene-benzoic acid-water, and benzene-propionic acid-water, the distribution coefficients being 0·068 and 2·76 respectively for the concentrations used in the experiments. Throughout benzene was used as the dispersed phase.

VOL. 1 1952

A few experiments have been made with methyl isobutyl ketone-benzoic acid-water where the distribution coefficient is 0·014.

The results obtained have been used to examine some previously reported data on perforated plate and spray towers.

EXPERIMENTAL WORK

Series 1. Transfer to forming drops

For precise measurement of the extraction occuring during drop formation, it would be desirable to analyse the drop immediately after it is formed. This is very difficult and the method adopted has been to form a drop on a jet in the continuous phase, and as soon as it is formed to push it out of the system. Two forms of equipment have been used as shown in Fig. 1 and 2, the first for conditions of slow formation of drops and the second for more rapid formation.

As shown in Fig. 2, the benzene phase flows from a small reservoir through a needle valve to form a drop at the end of the glass jet fixed in the base of the column holding the continuous phase. A side tube of $\frac{1}{2}$ mm i.d. is sealed just below the jet, so that if the two way cock is turned the flow of benzene is cut off and the drop is forced out of the system by the hydrostatic head of the continuous phase. The procedure was to set the needle valve to give the desired rate of drop formation and when the drop had reached the desired size as shown by a scale at the back of the tube, the cock was turned and the drop pushed out of the apparatus and collected in the burette as shown. This cycle was repeated until sufficient liquor had been collected for analysis, the liquor in the column being stirred after every ten drops. The drop volume was obtained from the number of drops and the total volume and time of drop formation were recorded. This method was only suitable for times of formation greater than 3 sec.

For more rapid drop formation the automatic apparatus (Fig. 2), was developed. Here the head of liquor in the column is balanced by an equivalent head on the inlet and outlet tubes. If the pressure at the top of the column is slightly reduced a drop will form on the jet, and when the pressure is increased again the drop will be forced out of the column. By the use of two ball valves the drop is drawn up the inlet tube, but is pushed back out of the side tube to the measuring burette. Drops were formed and removed by fluctuating the pressure at the top of the column using a small piston pump as shown. The pump was driven by a geared motor so that a wide range of rates of drop formation could be obtained ($\frac{1}{2}$ to 3 secs). By fitting a variable throw eccentric the actual drop volume could also be varied.

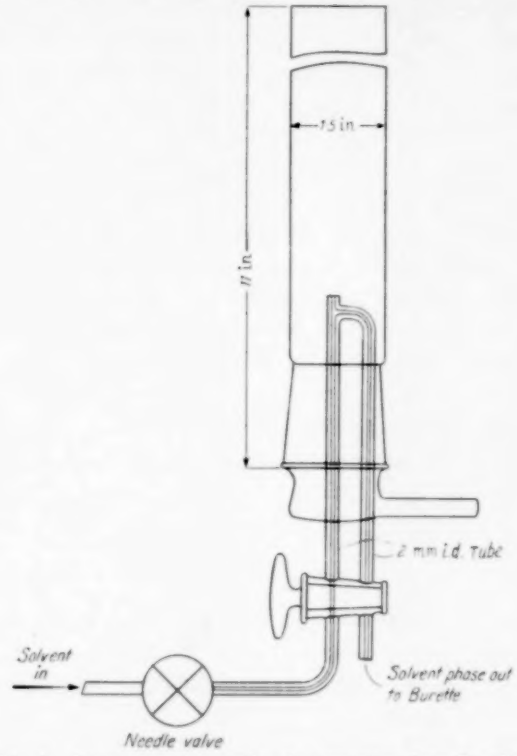

Fig. 1. Apparatus for study of extraction into forming drops.

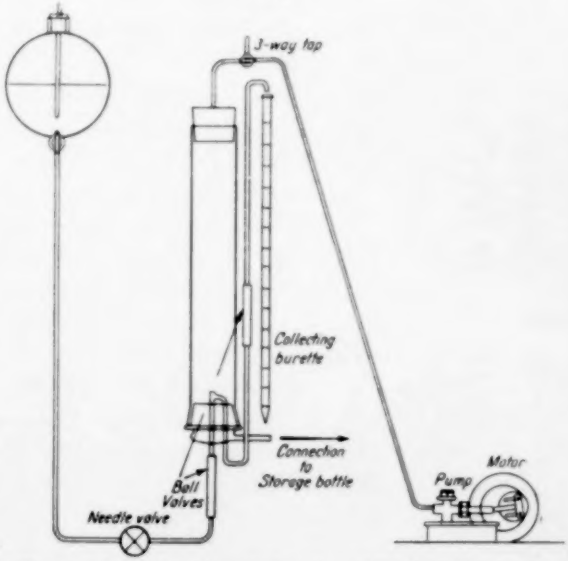

Fig. 2. Apparatus for study of rapidly forming drops.

Four sets of experiments Series 1 A–D were made at constant drop size, and varying rates of drop formation, and one set 1 E, with constant drop rate but varying drop size. In these tests benzoic acid was extracted from the water phase to the dispersed benzene drops. A further set 1 F was made using propionic acid as the solute. The analysis in all cases was accomplished by shaking the benzene sample with excess NaOH, and titrating the mixture with HCl, using thymol blue indicator. In all cases a blank titration was carried out with the same quantity of HCl and NaOH, and the benzene normality was obtained from the difference between the two titres.

Methods of calculation

The two quantities of greatest interest are:

1. The total extraction occuring during drop formation and withdrawal.

2. The rate at which the extraction takes place.

1. The amount of extraction—This is conveniently expressed as a percentage of the extraction that would be obtained if the drop attained equilibrium with the surrounding liquid.

$$i.e.\ \%\ \text{Equilibrium} = \frac{\text{Final normality} \times 100}{\text{Equilibrium normality}} \qquad (8)$$

where the normality of the collected drops is used as a measure of the concentration.

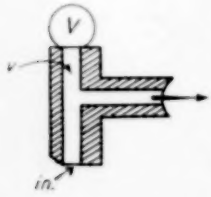

In the operation of the apparatus there is a small volume v above the withdrawal point which is filled with the dispersed liquid during drop formation. This liquid, however, does not enter the drop but is pushed out when the drop is collapsed. If V be the volume of the actual drop formed, then in each cycle a volume $(V + v)$ of liquor enters the apparatus from the dispersed liquor reservoir. This is the volume of liquor that is actually pushed out and measured in the burette, so that the percentage approach to equilibrium based on the volume V of the actual drop is E_v

$$E_v = \frac{\text{Final normality}}{\text{Equilibrium normality}} \cdot \frac{(V+v) \cdot 100}{100}. \qquad (9)$$

It is convenient to express all results for a constant concentration of the aqueous phase. H, for the system benzene-benzoic acid-water varies with concentration, and although for any one experiment the concentration change is very small, it is necessary to allow for the change in H throughout the experiments in any series as they were not carried out at precisely the same concentration.

For this system H/K_b is small compared with $1/k_w$, and we may take $K_w = k_w$. But k_w is dependent on the physical properties of the system and may be taken as constant over the concentration range considered. Hence we may take K_w as constant. Total extraction $\propto K_w$ (driving force in water phase). For dilute concentrations this driving force may be taken as equal to the actual concentration in the water phase.

Hence,

$$\text{Final benzene normality} \propto \text{Water phase normality} \qquad (10)$$

since the benzene normality represents the mass transferred.

The results in these series have been corrected to a water phase concentration of 0·011, for which value H equals 0·162. The corrected approach to equilibrium for these standard conditions will be:

$$E = \frac{\text{Final benzene normality}}{0{\cdot}162} \cdot \frac{(V+v)}{V} \times \frac{100 \times 0{\cdot}011}{\text{Water normality}}. \qquad (11)$$

This correction is very small and hardly necessary for forming drops, but is of greater importance for the experiments with rising drops. With propionic acid as solute H is sensibly constant and no similar correction is required.

2. The rate of extraction—With forming drops the interfacial area is continuously changing, but an average value may be calculated in the following way. First we must find an average time of exposure t_e for the drop that is formed and collapsed in a time t_f, the time of formation being equal to the time of collapse. Assume further that the volume of the drop increases uniformly with time and that the drop is spherical.

Let R be the radius of the drop at a time $\frac{1}{2}t_f$, when the drop is fully formed.

Let M be the volumetric rate of flow, so that the volume at time t is $M \cdot t$.

Let r be the radius at any time t, so that $M \cdot t = \frac{4}{3} \cdot \pi \cdot r^3$ and $dt = \dfrac{4 \cdot \pi \cdot r^2 \cdot dr}{M}$.

The interfacial surface at time t, $S = 4 \cdot \pi \cdot r^2$.

VOL. 1 1952

The average surface between 0 and t_f is given by,

$$S_{av} = \int_0^{t_f} \frac{4 \cdot \pi \cdot r^2 \cdot dt}{t_f}$$

$$= \int_0^R \frac{4 \cdot \pi \cdot r^2 \cdot 4 \cdot \pi \cdot r^2 \cdot dr}{M} \cdot \frac{3 \cdot M}{4 \cdot \pi \cdot R^3}$$

$$= \int_0^R \frac{12 \cdot \pi \cdot r^4}{R^3} \cdot dr = \frac{12 \cdot \pi \cdot R^2}{5}. \qquad (12)$$

The actual time of formation and collapse of the drop t_f is given by

$$t_f = \left(\frac{V}{V+v}\right) t_c \qquad (13)$$

where t_c is the measured time of one cycle during which a volume $(V+v)$ of liquor flows into and out of the unit.

If in any interval of time t to $t + dt$, a surface ds is formed then it will be exposed for a period $t_f - t$ during the cycle. Hence the average time of exposure t_e is given by

$$t_e = \frac{\int_0^{t_f} (t_f - t)\, ds}{\int ds}.$$

Noting that $M \cdot t = \frac{4}{3} \cdot \pi \cdot r^3$, so that $(t_f - t) = \frac{4 \cdot \pi \cdot (R^3 - r^3)}{3 \cdot M}$.

$$\int_0^{t_f} (t_f - t)\, ds = \int_0^R (t_f - t)\, 8 \cdot \pi \cdot r \cdot dr$$

$$= \int_0^R \frac{4 \cdot \pi}{3 \cdot M} \cdot (R^3 - r^3)\, 8 \cdot \pi \cdot r \cdot dr$$

whence $$t_e = \frac{\int_0^R \frac{32 \cdot \pi^2}{3 \cdot M} (R^3 \cdot r - r^4)\, dr}{\int_0^R 8 \pi \cdot r \cdot dr} = \frac{3}{5} t_f \qquad (14)$$

i.e. the average time of exposure is $\frac{3}{5}$ the time of formation and collapse. For the automatic machine the time of formation was equal to the time of collapse but this was not accurately so with the hand apparatus. Eq. (14) will, however, apply in both cases.

Using these relations the average coefficient of transfer can be expressed in terms of the average interfacial area exposed per unit time. The data for one run with benzoic acid are evaluated below.

Example calculation

Measured time for formation and collapse of drop t_c . . . . . 2 secs
Drop volume $V + v$ . . . . . 0·085 ml
Actual drop volume V . . . . . 0·067 ml
Final normality of drop sample . . . . . 0·00053
Water phase normality . . . . . 0·0116

$$\% \text{ Equilibrium } E = \frac{0{\cdot}00053 \times 0{\cdot}085 \times 0{\cdot}011 \times 100}{0{\cdot}162 \times 0{\cdot}067 \times 0{\cdot}0116} = 0{\cdot}39.$$

$$\text{Time for formation and collapse of drop} = 2 \times \frac{0{\cdot}067}{0{\cdot}085} = 1{\cdot}58 \text{ secs.}$$

Final radius of drop R, $\left| \frac{4 \cdot \pi \cdot R^3}{3} = 0{\cdot}067 \right| = 0{\cdot}021$ cms.

Average surface exposed $S_{av} = \frac{12}{5} \cdot \pi \cdot R^2 = 0{\cdot}48$ sq cms.

Since a normal solution of benzoic acid has 1 gm mole/litre, the moles of acid transferred to the dispersed phase

$$= \frac{0{\cdot}085 \quad 0{\cdot}00053}{1000}.$$

$$\text{Rate of transfer } \frac{0{\cdot}085 \quad 0{\cdot}00053 \times 3600}{1000 \quad 1{\cdot}58 \times 0{\cdot}48} = 0{\cdot}214 \times 10^{-3} \text{ gm mols/hr cm}^2.$$

The water phase concentration does not alter and may be taken as the driving force since the benzene phase initially had no benzoic acid.

Driving force $= 0{\cdot}0116 \times 10^{-3}$ gm mols/cc.

Hence the average transfer coefficient $K_w = \frac{\text{gm mols}}{\text{hr cm}^2} \times \frac{1}{\text{gm mol/cc}} = \frac{0{\cdot}214 \times 10^{-3}}{0{\cdot}0116 \times 10^{-3}}$

$= 18{\cdot}4$ gm mols/hr cm² (gm mol/cc).

Giving $K_w = 0{\cdot}61$ lb mol/hr ft² (lb mol/ft³).

Experimental results for transfer to forming drops

The experimental results are expressed by considering the influence of, time of drop formation and collapse t_f, the drop size, and the physical properties of the system on the rate of transfer and on the amount of transfer. A summary of the experimental data is given in Table 1.

1. Effect of time of drop formation and collapse t_f—The transfer effected E is shown plotted against t_f for the two systems in Fig. 3 and 4. The points for propionic acid lie on a smooth curve and although those for benzoic acid are more scattered a similar curve has been drawn through them. It is seen that E increases with t_f, but for values of $t_f > 5$, the increase is very small. E is numerically small for both systems, and since the total extraction increases very slowly with t_f, the rate of extraction must

Table 1. Benzene-benzoic acid-water.

Measured drop volume ml	*V* ml	*Average exposed interface* cm²	*Measured overall drop time* secs	*Actual overall drop time* secs	*Mean water normality* $\times 10^{-2}$	*Final benzene normality* $\times 10^{-4}$	% *Equilibrium*	K_w *gm mols/hr cm² (gm mols/cc)*	K_w *lb mols/hr ft² lb mols/ft²*
0·0685	0·0505	0·395	0·7	0·515	1·095	4·0	0·33	44·5	1·46
0·069	0·051	0·4	0·86	0·635	1·17	4·65	0·37	39	1·28
0·071	0·053	0·41	1·22	0·91	1·16	4·6	0·36	27·6	0·91
0·069	0·051	0·39	1·5	1·11	1·11	4·9	0·40	25·4	0·83
0·069	0·051	0·40	1·72	1·27	1·17	4·9	0·38	20·4	0·67
0·068	0·050	0·39	3·0	2·2	1·16	5·5	0·44	13·7	0·45
0·0887	0·0707	0·5	0·71	0·565	1·095	4·2	0·33	42	1·38
0·0835	0·0655	0·47	0·91	0·712	1·16	4·6	0·34	36·2	1·19
0·0845	0·0665	0·48	1·2	0·945	1·16	4·8	0·36	28	0·92
0·0846	0·0666	0·48	1·5	1·18	1·11	4·8	0·37	22·4	0·735
0·085	0·067	0·48	2·0	1·58	1·16	5·3	0·39	18·8	0·62
0·0864	0·0684	0·49	3·0	2·38	1·14	5·5	0·415	13·1	0·43
0·099*	0·081	0·54	9·25	7·57	1·15	5·95	0·625	6·5	0·212
0·109	0·091	0·59	0·87	0·73	1·10	4·5	0·334	36·6	1·2
0·118	0·100	0·62	1·08	0·915	1·18	4·4	0·3	28·6	0·935
0·120	0·102	0·63	1·52	1·29	1·18	4·8	0·326	22	0·72
0·123	0·105	0·645	2	1·71	1·18	5·5	0·37	19·3	0·63
0·114	0·096	0·61	2·6	2·22	1·08	5·2	0·39	15·5	0·51
0·129	0·111	0·67	1·52	1·31	1·135	4·9	0·34	23·2	0·76
0·131	0·113	0·675	1·98	1·71	1·135	5·5	0·38	20	0·66
0·127	0·109	0·66	3·1	2·66	1·135	5·7	0·39	13·2	0·435
0·134*	0·116	0·68	4·1	3·58	1·12	5·4	0·38	9·6	0·315
0·136*	0·118	0·69	9·15	7·95	1·13	7·4	0·514	5·85	0·192
0·138*	0·120	0·7	16·2	14·1	1·13	10·3	0·68	4·55	0·149
0·054	0·036	0·31	1·5	1·0	1·10	5·0	0·46	28·7	0·94
0·064	0·046	0·37	1·5	1·08	1·09	4·6	0·4	24·7	0·81
0·074	0·056	0·42	1·5	1·13	1·12	5·5	0·44	27·1	0·89
0·08	0·062	0·455	1·5	1·16	1·13	5·2	0·4	25·3	0·83
0·092	0·074	0·51	1·5	1·2	1·12	5	0·376	24	0·79
0·102	0·084	0·555	1·5	1·23	1·09	4·8	0·366	24	0·79
0·123	0·105	0·65	1·5	1·28	1·09	5·2	0·39	25·1	0·825

Table 1 (continued). Benzene-propionic acid-water

Measured drop volume ml	*Actual drop volume* ml	*Average exposed interface* cm²	*Measured overall drop time* secs	*Actual overall drop time* secs	*Mean water normality* $\times 10^{-2}$	*Final benzene normality* $\times 10^{-3}$	% *Equilibrium*	K_B *gm mols/hr cm² (gm mols/cc)*	K_B *lb mols/hr ft² lb mols/ft²*
0·095	0·0725	0·505	0·765	0·613	5·11	6·73	4·5	40	1·31
0·089	0·071	0·495	1·03	0·82	5·14	7·4	5·0	32	1·05
0·09	0·072	0·5	1·44	1·15	5·26	9·1	6·0	27·6	0·905
0·092	0·074	0·515	1·98	1·6	5·2	10·05	6·6	22	0·72
0·093	0·075	0·52	3·03	2·44	5·11	11·5	7·85	17·4	0·57
0·096*	0·078	0·53	4·24	3·44	5·2	12·6	8·3	13·2	0·433
0·095*	0·077	0·525	6·75	5·46	5·2	12·9	8·5	8·5	0·28
0·096*	0·078	0·53	10·8	8·8	5·2	16·3	10·65	6·8	0·224

* Indicates experiments with hand apparatus.

decrease very rapidly. This is shown quantitatively in Fig. 5 and 6, where the transfer coefficients K_w for benzoic acid and K_B for propionic acid are shown plotted against t_f. The points lie on reasonably good straight lines which may be expressed as:

$$K_w = 0{\cdot}89\ 1/t_f^{0{\cdot}7}$$ Benzene-benzoic acid-water

$$K_B = 0{\cdot}96\ 1/t_f^{0{\cdot}7}$$ Benzene-propionic acid-water

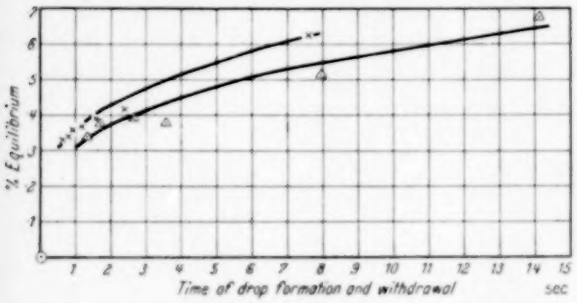

Fig. 3. Variation of extraction with time of drop formation (for drops of benzene forming in 0·011 N benzoic acid). Drop Volume × 0·07 ml; △ 0·114 ml.

It is of interest to compare these results with the HIGBIE theory which as mentioned was developed for the absorption of a pure gas into an infinite depth of liquid across a plane interface. According to this theory

$$k = 2\sqrt{\frac{D}{\pi t_e}}. \qquad (15)$$

Using a paper by WILKE [10], and assuming D_b/D_p a constant, for the solvents benzene and water, values of D have been calculated for 15° C.

D_{wb}	Benzoic acid in water	$2{\cdot}69 \times 10^{-5}$ ft²/hr
D_{Bb}	Benzoic acid in benzene	$5{\cdot}28 \times 10^{-5}$ ft²/hr
D_{wp}	Propionic acid in water	$3{\cdot}4 \times 10^{-5}$ ft²/hr
D_{Bp}	Propionic acid in benzene	$6{\cdot}66 \times 10^{-5}$ ft²/hr

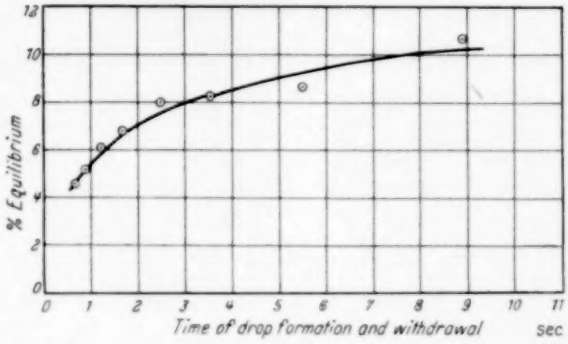

Fig. 4. Variation of extraction with time of drop formation (for drops of benzene forming in 0·52 N propionic acid).

Taking $t_e = 1$ (*i.e.* $t_f = 1{\cdot}67$) for benzoic acid system,

$$k_{wb} = 2\sqrt{\frac{2{\cdot}69 \times 10^{-5} \times 3600}{\pi}} = 0{\cdot}354 \qquad (16)$$

$$k_{Bb} = 2\sqrt{\frac{5{\cdot}28 \times 10^{-5} \times 3600}{\pi}} = 0{\cdot}492 \qquad (17)$$

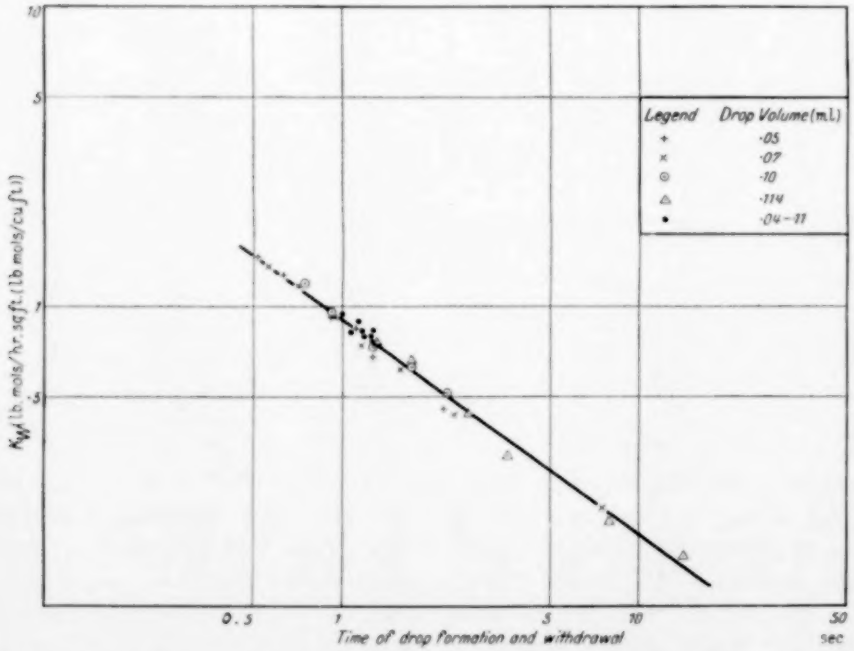

Fig. 5. Variation of K_w with time of drop formation (for drops of benzene forming in 0·011 N benzoic acid).

whence

$$\left.\begin{aligned}\frac{1}{K_{wb}} &= \frac{1}{0{\cdot}354} + \frac{0{\cdot}068}{0{\cdot}492}\\ &\text{giving } K_{wb} = 0{\cdot}34 \text{ lb mol/hr ft}^2 \text{ (lb mol/ft}^3\text{)}\\ \text{and}\\ \frac{1}{K_{Bp}} &= \frac{1}{0{\cdot}555} + \frac{1}{0{\cdot}39 \times 2{\cdot}8}\\ &\text{giving } K_{Bp} = 0{\cdot}37 \text{ lb mol/hr ft}^2 \text{ (lb mol/ft}^3\text{)}\end{aligned}\right\} \quad (18)$$

where K_{wb} is overall coefficient based on water phase concentration with benzoic acid as-solute.

The experimental values for drops formed and collapsed in 1·67 secs ($t_e = 1$ sec) are $K_{wb} = 0{\cdot}64$ and K_{bp} of 0·68, which are about twice those given

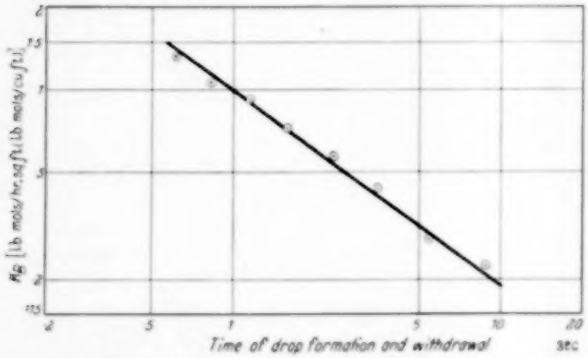

Fig. 6. Variation of K_B with time of drop formation (for drops of benzene [0·07 ml] forming in 0·52 N propionic acid).

by the HIGBIE theory. The index for the experimental work is $t_f^{-0{\cdot}7}$ whereas the theory gives $t_f^{-0{\cdot}5}$. It is difficult to give a satisfactory explanation for these differences but the actual process of drop formation may be more complex than appears and eddies may give rise to more rapid transfer.

2. Effect of drop size—The percentage equilibrium reached by the drop increases as the drop volume decreases. This is believed to occur because of the increased area of interface per unit volume with the smaller drops. For the range in drop volume examined (0·04–0·114 ml), the overall transfer coefficient was found to be constant, but the range is too small for any definite conclusions to be reached.

3. Effect of change of solute—The behaviour of both systems is basically similar, but with propionic acid as the solute the drops attain more closely to equilibrium with the water phase. The values of K for both systems are also similar. Since the resistance to transfer is in both phases with propionic acid as solute and mainly in the water film with benzoic acid as solute, the latter system might be expected to give the higher value of K. On the other hand the diffusivity of propionic acid in benzene is larger than that of benzoic acid in water, and it is believed that it is this difference in diffusivities that causes the differences in the film transfer coefficient for the two systems.

Transfer to rising drops. Series 2 and 3

Two series of experiments have been made in which the transfer to rising drops was measured. In series 2,

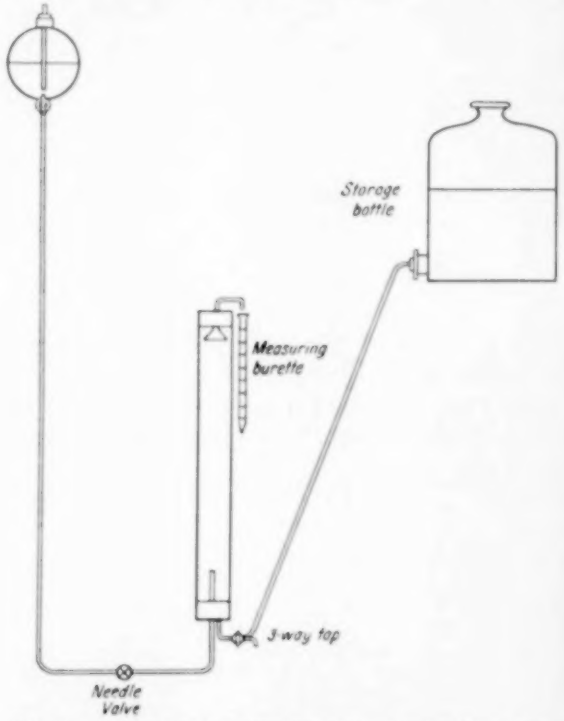

Fig. 7. Apparatus for measurement of extraction into rising drops.

the drops were formed from a glass jet and rose through a column containing the continuous phase at rest. In series 3, arrangements were made for the continuous phase to flow down the column countercurrent to the rising drops.

Series 2.

Transfer to single drops rising through still liquid

The glass apparatus used is illustrated in Fig. 7. The column was 1 in. diameter and was closed at the bottom by a rubber bung through which passed the glass jet. The phase to be dispersed was contained in a large funnel and passed via a stainless steel needle valve through the jet into the column. A

VOL. 1 1952

range of tubes of various heights were available and several jets were used to give drops of different size. The dispersed drops on reaching the top of the column were directed through the inverted funnel out of the column and into a burette. In operation the column was filled with the aqueous phase to the neck of the top funnel and the needle valve was adjusted to give the desired rate of drop formation. It was important to maintain the top interface at a fixed position inside the funnel to give reproducible end conditions.

The following factors were varied and their influence on the approach to equilibrium and on K were determined.

1. Time of rise of the drop.
2. Size of drop.
3. Rate of drop formation.
4. Physical properties and distribution relation for the system.
5. End effects.

To obtain the value of K for the period of rise of the drops, experiments were made with two columns of 33 and 125 cm high; by subtracting the results in the short tube from those in the long one, the end effects are largely eliminated, and K for the period of rise can be found. These experiments are conveniently arranged as:

Series 2 A–E Two heights of column with five jet sizes, using Benzene-benzoic acid-water.
F Three columns of differing diameter with the same jet size.
G Two heights of column with one jet using the system Benzene-propionic acid-water.
H As G but using Methylisobutylketone-benzoic acid-water.

Calculation of transfer coefficient K for rising drops

Using Benzoic acid as the solute the percentage equilibrium attained by the drop with the aqueous phase is very small, and taking the distribution coefficient as constant for any one test, K is given by,

$$K_w = \frac{N}{t \cdot S \cdot \Delta C_m} \qquad (22)$$

where N is the mols transferred in time t. It is, however, not so much the height of rise that is important but the actual time of rise. The method used can be set out as below for tests D where the time of drop formation was 1 sec and the drop volume 0·097 ml. (Interface = 1·015 sq. cm.)

Water phase conc. = 0·011 N

Time of rise secs	*Height of rise* cms	*E*	*Benzene normality*	*Equil. water normality*
12·05	125	4·225	0·0072	0·0018
3·2	33	1·725	0·0031	0·0011

$$\text{Hence } \Delta C_m = 0{\cdot}011 - \frac{0{\cdot}0018 + 0{\cdot}0011}{2} = 0{\cdot}00955$$

and
$$K_w = \frac{2{\cdot}5 \times 0{\cdot}162 \times 0{\cdot}097 \times 3600}{1{\cdot}015 \times 0{\cdot}00955 \times 8{\cdot}85}$$
$$= 16{\cdot}3 \text{ gm mols/hr cm}^2 \text{ (gm mols/cc)}$$
or
$$K_w = 0{\cdot}535 \text{ lb mol/hr ft}^2 \text{ (lb mol/ft}^3\text{)}.$$

The experimental results are presented in a series of tables and figures which are discussed below.

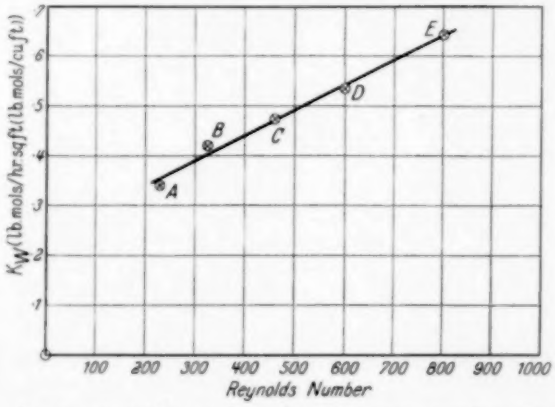

Fig. 8. Variation of K_w with Reynolds number (for drops of benzene rising through 0·011 N benzoic acid; height of rise 33–125 cm).

The influence of the time of rise of the drops is brought out together with the size of the drops since this latter factor alters the velocity of rise and K_w is determined by the difference in extraction over the two heights of 33 and 125 cms.

Effect of drop size on K for rising drops. Series 2 A–E

Fig. 8 shows the values of K_w plotted against Re based on the physical properties of the continuous phase and the drop diameter, and Fig. 9 values of K_w and the drop diameter. The averaged values for each series are given in Table 2 which shows the drop diameter and the velocity of rise. The values of K_w have been determined as explained and only refer to the period of rise.

Table 2. Experiments: Series 2 A–E

Variation of K_w with drop size for rising drops. System Benzene-benzoic acid-water with 0·011 N Benzoic acid as water phase.

Series	Drop volume ml	Drop diameter mm	Velocity of rise cm/sec	Re	K_w lb mols hr ft² (lb mols/ft³)
2 A	0·0136	2·96	7·7	228	0·34
2 B	0·026	3·68	8·75	322	0·42
2 C	0·048	4·52	10·2	460	0·475
2 D	0·097	5·7	10·45	600	0·535
2 E	0·260	7·92	10·6	840	0·645

Since an increase in the drop size does not of itself alter any of the factors on which K is based,

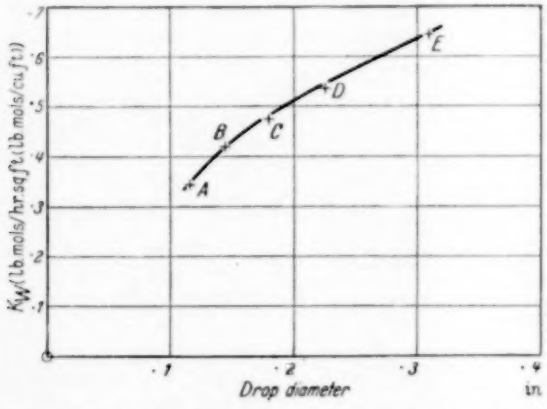

Fig. 9. Variation of K_w with drop diameter (for drops of benzene rising through 0·011 N benzoic acid; height of rise 33–125 cm).

the increase in K with Re must be attributed to alteration of the flow conditions around the drop. The points on Fig. 8 lie on a straight line, whilst those of Fig. 9 lie on a curve. This arises from the fact that with very small drops the velocity of rise is less than with the larger drops and the Re group allows for this factor. For very low values of Re the drop should behave as a solid sphere and the flow around it should be streamline. On this basis a rapid falling off of the curve in Fig. 9 is expected for low values of Re.

Effect of rate of drop formation on transfer

The results of series 2 D are given in Table 3, from which it is seen that there is no significant effect of the rate of formation of the drop on the transfer occuring during rise. The total transfer will be affected

Table 3. Experiments: Series 2 D

Effect of time of drop formation on mass transfer to rising drops. System Benzene-benzoic acid-water. yet diameter 1·24 mm.

Time of drop formation secs	Time of rise secs	Drop volume ml	Final benzene normality	Water normality	% Equilibrium
Column height 33 cm					
0·5	3·2	0·085	0·00276	0·0111	1·68
0·52	3·2	0·081	0·00278	0·0111	1·7
0·74	3·2	0·092	0·00276	0·0111	1·68
0·83	3·2	0·083	0·0024	0·0111	1·46
1·6	3·2	0·086	0·00295	0·0111	1·8
2·3	3·2	0·098	0·00286	0·0111	1·74
3·15	3·2	0·097	0·00306	0·0111	1·86
Column height 125 cm					
0·59	12	0·091	0·0062	0·0113	3·72
0·6	12·2	0·086	0·0076	0·0113	4·55
0·7	12	0·0875	0·0069	0·0113	4·13
1·35	12	0·094	0·0073	0·0113	4·37
2·22	12·2	0·098	0·0070	0·0113	4·2
2·42	12	0·097	0·0074	0·0113	4·43
3·56	12	0·099	0·0075	0·0113	4·52

since the transfer during drop formation is influenced by the time of drop formation.

Effect of distribution coefficient and solute diffusivity. 2 G

The method used for calculating the extraction coefficients for the system benzene-propionic acid-water was similar to that described above excepting that the drops approached more closely to equilibrium, and the extraction across the top interface was different in the 35 cm column from that in the 125 cm column. The transfer was assumed proportional to the concentration at the top and the results were obtained by successive approximations.

Results for the tests with 33 and 125 cm columns are given in Table 4. For a drop volume of 0·072 ml $K_w = 0·5$ for benzoic acid and $K_B = 0·525$ with propionic acid. These values for rising drops are related to each other much in the same way as those given earlier for forming drops.

Effect of interfacial tension

To investigate the effect of a marked change in the interfacial tension the system methyl *iso*butyl-ketone

VOL. 1 1952

Table 4. Experiments: Series 2 G and H

Values of K_w for rising drops.
Tests G. System Benzene-propionic acid-water.
Tests H. System Methyl *iso*butyl ketone benzoic acid-water.

Tests	*Drop volume* ml	*Drop diameter* mm	*Velocity of rise* cm/sec	*Re*	K_w gm mols / hr cm² gm mol/cc	lb mol/hr ft² / lb mol/ft³
G	0·072	5·16	10·4	560	16·1	0·53
H	0·046	4·4	9·5	440	49·4	1·62

benzoic acid-water was studied. In this case E is very small and K_w is calculated as on p. The experimental results are given on Table 4. With both the systems methyl *iso*butyl ketone benzoic acid-water and benzene-benzoic acid-water the distribution coefficient is very low and most of the resistance will lie in the water phase. One would therefore expect similar values for K_w. The experimental values for K_w with methyl *iso*butyl-ketone as the solvent are, however, three times those with benzene. These differences cannot be explained on the existing simple ideas of diffusion and other factors must be involved. The interfacial tension between M. I. K. and water is only 8·8 dynes/cm while for benzene-water it is 35 dynes/cm. This is a large difference and may be the cause of the big difference in K_w for the two systems. Further evidence on the influence of interfacial tension will be given in Part 2.

Studies of the wall effect. Series 2 F

In the experiments the columns used were of sufficiently small diameter relative to the drop to influence to some extent the velocity of rise of the drop. It was therefore decided to investigate the effect of tube size in relation to the drop diameter. The results as given in Table 5 show clearly that K is independent of the tube size for drops of the same diameter. The drop as it rises through its own height displaces an equal volume of the continuous phase between itself and the tube wall and the relative velocity between the drop and the continuous phase is unaltered, although its absolute velocity is reduced.

Table 5. Experiments: Series 2 F

Studies of the wall effect.
System Benzene-benzoic acid-water.
Drop diameter 5·5 mm.

Column cm	*Diameter* in.	*Velocity of rise* cm/sec	*Velocity of rise* ft/hr	K_w lb mol/hr ft² / lb mol/ft³
1·1	0·39	6·74	895	0·505
1·5	0·59	8·25	975	0·49
3·0	1·18	10·6	1250	0·47
3·0	1·18	10·4	1230	0·52

K_w calculated using data for end effects given in Table 6.

Calculation of end effects

Some indication of the end effects can be obtained by calculating the anticipated extraction for a rise of 0–33 cm in 3·2 secs, based on K_w obtained for the rising section only, and comparing this value with the experimental figure.

For a period of rise of 8·85 secs (p. 205)

$$E = 2{\cdot}5 .$$

Hence for a period of rise of 3·2 secs, the expected value of E is

$$\frac{2{\cdot}5 \times 3{\cdot}2}{8{\cdot}85} = 0{\cdot}91 .$$

The experimental figure for this transfer is $E = 1{\cdot}725$, so that the end effects give rise to a value of $0{\cdot}81\,E$, or nearly 47% of the total transfer occuring in the column of 33 cm. If corrections are made for the small change in driving force between the section 0–33 cm and 33–125 cm, it can still be shown that the end effects amount to about 40% of the total transfer for the 33 cm column. A summary of these results is given in Table 6.

Table 6. Experiments: Series 2 C–E

Summary of end effects for mass transfer to rising drops.
System Benzene-benzoic acid-water.

Time of drop formation	*1 sec*	*2 sec*	*3 sec*
Series 2 C: Jet 0·78 mm			
Drop volume ml. . .	0·049	0·05	0·0495
% Equilibrium for formation .	0·405	0·47	0·525
% Equilibrium for both ends .	1·0	1·1	1·15
Factor R	2·4	2·3	2·2
Series 2 D: Jet 1·24 mm			
Drop volume	0·0955	0·098	0·097
% Equilibrium for formation .	0·33	0·38	0·41
% Equilibrium for both ends .	0·76	0·89	0·98
Factor R	2·3	2·3	2·3
Series 2 E: Jet 3·65 mm			
Drop volume ml. . .	0·29	0·275	
% Equilibrium for formation .	0·23	0·27	
% Equilibrium for both ends .	0·41	0·6	
Factor R	2·1	2·2	

$$R = \frac{\text{Combined end effects}}{\text{Transfer during drop formation}} .$$

Series 3.

Extraction into drops rising through a moving liquor

In a number of practical examples of extraction the drops rise against a falling stream of the continuous phase. These conditions have been produced using

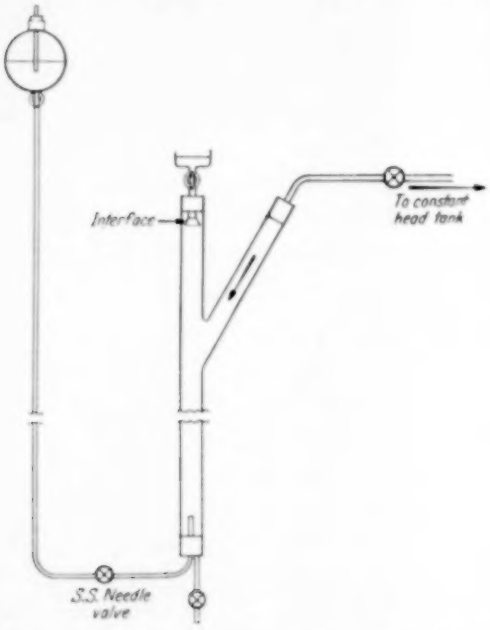

Fig. 10. Apparatus for measuring mass transfer into drops rising through a moving continuous phase.

the apparatus shown in Fig. 10. The flow of the continuous phase was controlled by the stainless steel valve and the interface maintained in the neck of the funnel at the top. The drops were collected in a small reservoir above the column. In operation the continuous phase was first started, and when it was flowing at the desired rate the dispersed phase was introduced. The experiments were made with the system benzene-benzoic acid-water, and the time of drop formation kept constant at 2 secs.

The results are presented in Table 7, which gives the mean downward velocity of the continuous phase, the absolute velocity of rise of the drops and the total time of rise. Under these conditions, *Re* based on the relative velocity of the two phases and the drop diameter does not alter, any increase in the downward velocity of the continuous phases being equivalent to a decrease in the upward velocity of the drop. The important effect of an increase in the downward velocity of the continuous phase is that it increases the time of contact of the drop with the liquid for a given height of rise. Thus the results are conveniently expressed for this series by plotting the approach to equilibrium against the time of contact, as shown in Fig. 11. This graph indicates that E varies with the time of contact of the two phases.

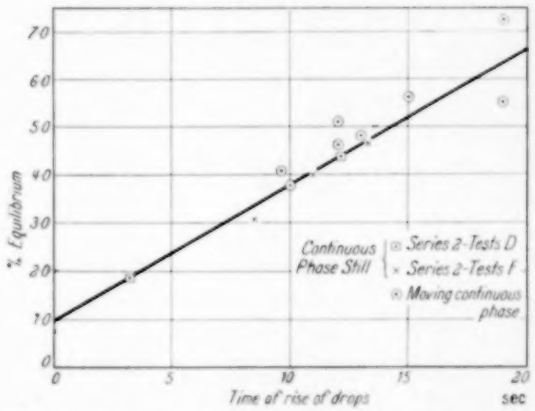

Fig. 11. Graph of % equilibrium vs. time of contact (for drops of benzene rising through moving liquid).

Fig. 11 also brings out the fact that the actual transfer is increased equally by increasing the height of the column with zero flow

Table 7. Experiments: Series 3

Effect of velocity of continuous phase on transfer to rising drops.
System Benzene-benzoic acid-water.
Jet diameter 0·114 mm.
Height of moving column 80 cms.

Time of drop formation secs	*Time of rise* secs	*Drop velocity* cm/sec	*Water velocity* cm/sec	*Drop volume* ml	*Water normality*	*Final benzene normality*	*E*
2·2	10	10	0	0·084	0·0116	0·0064	3·76
2·25	9·6	10·5	0	0·09	0·0117	0·007	4·06
1·95	12	8	1·98	0·085	0·0109	0·0074	4·5
1·8	12	8	2·2	0·101	0·0108	0·0081	5·1
2·02	13	7·3	3	0·101	0·0109	0·0077	4·8
1·7	15	6·15	4·2	0·104	0·0112	0·0092	5·6
2·03	19	4·7	5·2	0·118	0·0115	0·0112	7·23
2·15	19·6	4·55	5·35	0·116	0·0106	0·0086	5·5

VOL. 1 1952

of the continuous phase or by increasing the time of contact to the same extent by increasing the downward velocity of the continuous phase. Since ΔC_m and the drop volume are approximately constant the linear relationship between E and the time of contact is an indication that the transfer coefficient is independent of the latter.

Mechanism of mass transfer to rising drops

The results of the experimental work show that:

(1) K is independent of the time of contact.

(2) K increase with increasing drop size.

(3) K increases with decreasing interfacial tension.

(4) For the systems tested, K for a rising drop corresponds with K for a drop forming in a given time, irrespective of solute.

Consider the interface of the rising drop. At any time, t, a point, A, on the interface of the drop, a

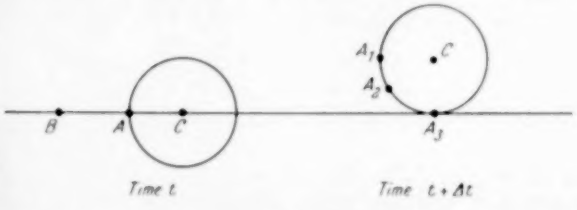

point, B, in the surrounding medium, and C, the centre of the drop are in the same horizontal plane. At a time, $t + \Delta t$, there are three possible positions for point A in relation to B and C.

(1) A and C remain in the same position relative to each other, the drop behaving as a solid sphere.

(2) A remains in the same position relative to B (A_3) in the diagram. For this to occur, A must move downwards relative to the drop centre at a velocity equal to the velocity of rise of the drop. The drop interface is therefore being continually formed at the top of the drop and destroyed at the bottom. Thus, the interface will be replaced every time the drop rises through its own height.

(3) A moves to some point, A_2, between A_1 and A_3. The drop is continually renewing its interface, but the tangential velocity at the equator of the drop is less than the velocity of rise.

Case (1) was considered by SHERWOOD [7], who showed that the predicted extraction was much smaller than the practical results. If we take the case of propionic acid, where the water phase resistance may be neglected, then the anticipated extraction may be calculated by NEWMAN'S method [12].

Thus,

$$\frac{W - C_e}{C_0 - C_e} = \frac{6}{\pi^2} \sum_{1}^{\infty} \frac{1}{n^2} \cdot e^{-\frac{n^2 \cdot \pi^2 \cdot D\theta}{a^2}}$$

θ = time of formation and rise (secs);

a = radius of drop;

W = mean concentration within drop;

n = an integer number.

For a time of drop formation and rise of 14 secs (Tests G) $D_{bp} = 1{\cdot}72$ cm²/sec.

$$\frac{D\theta}{a^2} = \frac{1{\cdot}72 \times 14 \times 10^{-5}}{0{\cdot}26^2} = 0{\cdot}00356.$$

Drop diameter = 0·52 cm (Table 4).

From NEWMAN'S paper, the corresponding value of $\frac{W - C_e}{C_0 - C_e}$ is 0·81. This gives the predicted equilibrium as 19%, whereas the experimental figure is 55%, or nearly three times as much. If the water phase resistance were included the difference would be greater.

In examining case (2), we may apply HIGBIE'S equation

$$k = 2\sqrt{\frac{D}{\pi \cdot t_e}}$$

for a velocity of rise of 10·4 cm/sec.

Diameter of drop = 0·52 cm.

$$k_b = 1{\cdot}13\sqrt{\frac{1{\cdot}72 \times 10^{-5}}{0{\cdot}05}}$$

$$= 2{\cdot}1 \times 10^{-2} \text{ gm mols/hr cm}^2 \text{ (gm mols/cc)}$$

$$= 2{\cdot}5 \text{ lb mols/hr ft}^2 \text{ (lb mols/ft}^3\text{)}$$

$$k_w = 1{\cdot}13\sqrt{\frac{0{\cdot}88 \times 10^{-5}}{0{\cdot}05}}$$

$$= 1{\cdot}5 \times 10^{-2} \text{ gm mols/hr cm}^2 \text{ gm mols/cc)}$$

$$= 1{\cdot}78 \text{ lb mols/hr ft}^2 \text{ (lb mols/ft}^3\text{)}$$

whence

$$\frac{1}{K_B} = \frac{1}{2{\cdot}5} + \frac{1}{2{\cdot}76 \times 1{\cdot}78}$$

or

$$K_B = 1{\cdot}66 \text{ lb mols/hr ft}^2 \text{ (lb mols/ft}^3\text{)}.$$

This result is three times the experimental figure, which lies between case (1) and (2). Thus, the mechanism may be considered as represented by case (3), in which the drop renews its interface as it rises, but that the tangential velocity of the interface is less than the velocity of rise. The rate of interface formation per unit of interface would be expected to decrease with drop size and increase with decreasing interfacial tension. The general results are in agreement with these two features.

Application of data for single drops to spray and perforated plate towers

The experiments so far described have provided data on the extraction occuring during formation, rise and coalescence of the drops as the top interface. These three stages form the basis of the operation of spray and perforated plate towers, and it is therefore of interest to examine the performance of such equipment in the light of the data obtained.

ALLERTON, STROM and TREYBAL [1], have published their results on the system toluene-benzoic acid water using a perforated plate column of the following construction.

Overall tower height . . . . . 5 ft 3½ in.
Internal diameter . . . . . 3·63 in.
Cross sectional area . . . . . 0·0719 ft² or 66·6 cm².

Plates 11. Thickness 1/16 in. Spacing 4·75 in. Holes 3/16 in. diameter. No. per plate 51. Disengaging space at top 7·625 in.

In operation the extraction was from toluene to the water, the toluene entering at the bottom. Since the distribution coefficient for benzoic acid in benzene/water is 0·068 and for toluene/water is 0·070 and the physical properties of the two systems are very similar the present data for benzene drops will be applied to examine the toluene system in the plate column described above.

Total height of column $= 4{\cdot}75 \times 11 + 7{\cdot}625 = 59{\cdot}875$ in.

Effective volume of column $= 0{\cdot}0719 \times \frac{59{\cdot}875}{12} = 0{\cdot}358$ ft³.

Flow rates: Toluene 57 ft³/ft² hr = 4·1 ft³/hr = 32 cc/sec.

Time of drop formation $= \frac{51 \times \text{Drop volume}}{32}$

$= \frac{51 \times 0{\cdot}37}{32} = 0{\cdot}59$ secs *.

Water 75·6 ft³/ft² hr $= 5{\cdot}44$ ft³/hr $= 42{\cdot}6$ cc/sec.

The transfer coefficient for the three stages of formation rise, and coalescence can now be calculated and hence the overall transfer coefficient deduced and compared with the experimental value given by ALLERTON.

Forming drops—For a drop of 0·37 ml forming in 0·59 secs K_w can be obtained from Fig. 5 as 1·3 lb mols/hr ft².

Average interfacial area of 1 drop . . . 1·49 cm²

Total area of forming drops on one plate $\frac{1{\cdot}49 \times 51}{30{\cdot}5^2} = 0{\cdot}082$ ft²

Total area of forming drops in columns $= 0{\cdot}082 \times 11 = 0{\cdot}902$ ft²

$(K \cdot S)_f$ forming drops $= 1{\cdot}3 \times 0{\cdot}902 = 1{\cdot}17$.

* Obtained from data for drop volume vs. time for formation for $\frac{5}{16}$" holes.

Rising drops—Allow as top interface at each plate a layer of ¾ in. as given by authors.

Velocity of drop in still water . . . . 13 cm/sec
Velocity of water phase 42·6/66·6 . . 0·64 cm/sec
Actual velocity of rise of drop . . . 12·4 cm/sec
Time of rise for 1 ft . . . . . 2·46 secs.

But height of column of rising drops $10 \times 4 + 7{\cdot}625 = 47{\cdot}62$ in.

Total time of rise $= \frac{47{\cdot}62 \times 2{\cdot}46}{12} = 9{\cdot}8$ secs.

No. of drops $\frac{9{\cdot}8 \times 51}{0{\cdot}59} = 845$.

Hence total area of rising drops $S_R = \frac{845 \times 2{\cdot}49}{30{\cdot}52} = 2{\cdot}26$ ft².

But K_w for rising drops of 0·37 ml at 12·4 cm/sec can be read from Fig. 9 as 0·69 lb mols/hr ft².

Hence $(K \cdot S)_R$ rising drops $= 2{\cdot}26 \times 0{\cdot}69 = 1{\cdot}56$.

Top interface—For drops of this size the tranfer occuring at the top of each plate may be taken as equal to that in formation (see Table 6).

The overall transfer coefficient as measured for the whole tower is then given by:

$$K_w \cdot a \cdot V = K_f \cdot S_f + K_r \cdot S_r + K_t \cdot S_t$$
$$K_w \cdot a \times 0{\cdot}358 = 1{\cdot}17 + 1{\cdot}56 + 1{\cdot}17 = 3{\cdot}90$$
$$K_w a = 10{\cdot}9 \text{ lb mol/hr ft}^3 \text{ (lb mol/ft}^3\text{)}.$$

Similar calculations have been made for two other flow rates and the results together with the experimental value of TREYBALL are given in the table,

Toluene flow ft³/ft² hr	*Water flow ft³/ft² hr*	$K_w \cdot a$ *calculated*	$K_w \cdot a$ *experimental*
38·6	36·4	9·1	7·8
57	76·5	10·9	11·2
79·7	65·8	15	18·1

Similar calculations have been made on the data of TREYBAL and DUMOULIN [9], using a perforated plate column very similar to that described above but in which the plate spacing could be varied. For three different flow rates, the values of $K_w a$ were 12·6, 7·4 and 7·4, whilst the calculated value based on this research was 12·7, 8·7, and 8·2. These calculated values are in very good agreement with the experimental values and it seems reasonable to conclude that the columns do in fact behave much as indicated by this work on individual drops.

SUMMARY

The extraction occuring from a continuous phase to dispersed drops has been measured both for conditions where the continuous phase is stationary and

VOL. 1 1952

when it is flowing countercurrently to the drops. The three stages of transfer have been measured directly, that during drop formation, that during the rise of the drop, and finally that occurring at the top interface of a column where the drops coalesce.

Mass transfer to a drop during formation has been found to be almost independent of the time of formation of the drop for a range of from $\frac{1}{2}$ to 1 sec for formation. The overall transfer coefficient K based on the average area exposed during formation of the drop decreases with increasing time of formation, but is practically independent of the drop size. Smaller drops approach more closely to equilibrium because of the increased area of interface per unit volume.

K for transfer during the rise of the drops has been found to increase with drop size, decrease with increasing interfacial tension, and is directly influenced by the relative velocity of the drops and the continuous phase. It is the time of contact rather than the height of rise that is important. Comparison of the experimental work with the anticipated results assuming the drops to rise as solid spheres or alternatively that they renew their surface each time they rise through one diameter suggests that the real conditions lie between these two cases. It is, however, felt that the reformation of the interface together with any recirculation of the liquor inside or around the drop that is the determining feature in the process. For a further understanding of the mechanism of the process measurements on the velocity of the interface are required. This is very difficult with drops but in Part 2 of this work the effect of the velocity of the interface in a horizontal extractor with the two streams flowing side by side in a tube will be discussed.

Acknowledgement—The authors wish to express their gratitude to Professor D. M. NEWITT F.R.S., in whose laboratories the work was carried out, for his guidance and encouragement at all stages. One of us also wishes to thank the *Department of Scientific and Industrial Research* whose grant made the work possible.

NOTATION

a = Area of interface per unit volume of apparatus (eq. 5)
C = Concentration of diffusing solute (mols/ft³)
C_a = Concentration of diffusing component in phase A (mols/ft³)
C_b = Concentration of diffusing component in phase B (mols/ft³)
C_{ai}, C_{bi} = Concentration of diffusing component at the interface in phases A and B
C_a^* = Concentration of diffusing component in phase A in equilibrium with concentration C_b in phase B
C_b^* = Concentration of diffusing component in phase B in equilibrium with concentration C_a in phase A
C_e = Concentration of absorbed gas in liquid phase under equilibrium conditions
C_0 = Initial concentration of gas in liquid phase
ΔC_m = Logarithmic driving force in concentration units
D = Diffusion coefficient (normally in ft²/hr)
E = Percentage approach to equilibrium
H = Ratio of concentration of solute in equilibrium in both phases
$k_a k_b k_L$ = Film transfer coefficients. mols/hr. unit area. (unit concentration difference)
k_w = Film transfer coefficient based on concentration in the aqueous phase
K = Overall transfer coefficient lb mols/hr ft² (lb mols/ft³
K_w = Overall transfer coefficient based on aqueous phase concentrations lb mols/hr ft² (lb mols per ft³)
K_a, K_b = Overall transfer coefficient based on concentrations in phase A and phase B respectively. Subscripts w and B denote water and benzene respectively.
N = Mols of diffusing component transferred
t = Time (normally in hrs)
t_e = Time of exposure of interface
t_f = Time of formation and collapse of drop
t_c = Time of one cycle for liquid to enter and leave drop apparatus
R = Radius of drop
S = Area of interface
v = Volume of liquor fed to jet that does not enter the drop
V = Volume of drop

REFERENCES

[1] ALLERTON, J., STROM and TREYBAL, R. E.; Trans. Amer. Inst. Chem. Eng. 1943 **39** 361. [2] ELGIN, J. C. and BROWNING, F. M.; *ibid.* 1935 **31** 639. [3] FALLAH, R., HUNTER, T. G. and NASH, A. W.; J. Soc. Chem. Ind. 1934 **53** 369 T and 1935 **54** 49 T. [4] HIGBIE, R.; Trans. Amer. Inst. Chem. Eng. 1935 **31** 365. [5] LICHT, W. JR. and CONWAY, J. B.; Ind. and Eng. Chem. 1950 **42** 1151. [6] ROW, S. B., KOFFOLT, J. H. and WITHROW, J. R.; Trans. Amer. Inst. Chem. Eng. 1941 **37** 559. [7] SHERWOOD, T. K., EVANS, J. E. and LONGCOOR, J. V. A.; *ibid.* 1939 **35** 597. [8] TREYBAL, R. E. and WORK, L. T.; *ibid.* 1942 **38** 203. [9] TREYBAL, R. E. and DUMOULIN; Ind. and Eng. Chem. 1942 **34** 709. [10] WILKE, C. R.; Chem. Eng. Prog. 1949 **45** 218. [11] WEST, F. B., *et al.*; Ind. and Eng. Chem. 1951 **43** 234. [12] NEWMAN, A. B.; Trans. Amer. Inst. Chem. Eng. 1931 **27** 203 and 310.

Heat transfer to fusible solids

T. K. Ross

(Received 1 April 1952)

Summary—The conditions of heat transfer to a fusible solid in contact with a heated surface are examined. A theoretical equation for the heat transfer coefficient is deduced, and compared with practical results. A shorter, empirical formula is suggested for design purposes.

Résumé—Etude de la transmission de la chaleur entre une surface chaude et un solide fusible.

Etablissement théorique d'une formule donnant le coefficient de transmission et comparaison avec les résultats expérimentaux.

L'auteur recommande l'emploi d'une formule empirique simplifiée, suffisante pour la pratique industrielle.

Although the problem of heat transfer to fusible solids arises in process design, the literature contains few references to the subject. Mathematical solutions of special cases have been provided by several authors [1], but practical investigations have apparently been limited to instances of ice formation [2], or of solidification and fusion on immersed surfaces [3].

A fusible solid may be melted by one of the following methods:

(a) The solid may be added to a mass of already molten material in a heated, agitated vessel.

(b) The solid may be arranged so that hot gases (or its own superheated vapour), may be circulated over it, the molten portion draining away.

(c) The solid may be placed on a heated surface, and the molten material drained away.

In case (a) once enough liquid has been accumulated in the vessel, the heat transfer is via this liquid. Hixson and Baum [4] have shown in their studies of mixing how this problem may be solved by correlation of the agitation, and physical properties of the system.

In (b) the heat necessary to raise the solid to melting point, and to bring about the fusion must be transferred through the gas film and liquid film successively. Work on this mechanism is in progress.

In example (c), the sensible and latent heats must be transferred from the hot surface to the melting solid through the film of molten matter. It is this problem which is examined here.

The liquid film

The condition of a film of liquid between two plane surfaces has been investigated, for example by Mitchell [5]. The present case is somewhat complicated by the fact that the fluid is not introduced along any preferred direction, but is generated at the solid surface. In general, however, the conditions of flow in such a film will be controlled by the viscosity and density of the liquid, the inclination of the film to the vertical, and the pressure exerted on the film by the weight of melting solid.

Then, the difference between the frictional forces at the boundaries of a small layer of the film (of thickness dx, and distant x from one face) must balance the accelerative forces when the flow rate is constant.

Thus

$$\mu \cdot \frac{dV}{dx} - \mu \cdot \frac{d(v+dV)}{dx} = g(\sigma + \varrho \cos\Theta) \cdot dx$$

for unit breadth and so,

$$-\mu \cdot \frac{d^2V}{dx^2} = g(\sigma + \varrho \cos\Theta) \cdot dx.$$

If there is no slip at either the heated surface or that of the melting solid, and if the latter is also stationary, integration gives

$$dV = g(\sigma + \varrho \cos\Theta)\left(m \cdot \frac{dx}{2} - x \cdot dx\right)$$

where "m" is the total film thickness.

Substituting the mass flow rate at any point, (dW/dt), for the velocity term, and integrating over the film results in the expression

$$m^3 = \frac{12\mu}{g\varrho(\sigma + \varrho\cos\theta)} \cdot \left(\frac{dW}{dt}\right). \qquad (1)$$

Heat transfer through the film

The flow of heat through the film covering a small portion of the heating surface, dA, may be written as

$$\frac{dQ}{dt} = h \cdot dA \cdot (T_s - T_m) \qquad (2)$$

so that

$$h = \frac{dQ}{dt \cdot dA \cdot (T_s - T_m)} = \frac{dQ}{dt \cdot B \cdot dL \cdot (T_s - T_m)},$$

when the surface has constant width B. If the liquid flow rate at this point is dW/dt also

$$\frac{dQ}{dt} = \frac{dW}{dt} \cdot [\lambda + C_p(T_m - T)] \qquad (3)$$

Combining (2) and (3)

$$h = \frac{dW\,[\lambda + C_p\,(T_m - T)]}{dt\,.\,B\,.\,dL\,.\,(T_s - T_m)} = \frac{k}{m} \qquad (4)$$

if the flow is viscous.

This expression is comparable to that developed by NUSSELT [6] for condensate films, and a similar process of integration over the entire surface results in the following expression for the mean film coefficient, h_m.

$$h_m = 0{\cdot}666\left[\frac{k^3 g\,\varrho\,(\sigma + \varrho\cos\theta)\,[\lambda + C_p\,(T_m - T)]}{\mu\,.\,L\,.\,(T_s - T_m)}\right]^{0{\cdot}25} \qquad (5)$$

or, in dimensionless form,

$$\frac{h_m\,.\,L}{k} = 0{\cdot}666\left[\frac{L^3 g\,\varrho\,(\sigma + \varrho\cos\theta)\,[\lambda + C_p\,(T_m - T)]}{k\,.\,\mu\,.\,(T_s - T_m)}\right]^{0{\cdot}25}. \qquad (6)$$

If the heating surface is provided as a horizontal tube, of outer diameter D_o, L becomes $\frac{\pi D_o}{4}$ and θ has a minimum value of 0°, so the alternative formula is then

$$\frac{h_m\,.\,D_o}{k} = 0{\cdot}710\left[\frac{D_o^3 g\,\varrho\,(\sigma + \varrho\cos\theta)\,[\lambda + C_p\,(T_m - T)]}{k\,.\,\mu\,.\,(T_s - T_m)}\right]^{0{\cdot}25}. \qquad (7)$$

Now eqs. (5), (6) and (7) apply only when the flow in the film is viscous, and the conditions for turbulence will now be examined. For turbulence to develop, on a plane surface,

$$Re > 2100 < \frac{4m\,B\,.\,dW}{2(m+B)\,.\,dt\,.\,m\,B\mu} = \frac{2}{B\mu}\left(\frac{dW}{dt}\right),$$

when m is small,

$$\text{or} \qquad \frac{dW}{dt} \quad \text{must exceed} \quad 1050\,B\mu\,. \qquad (8)$$

The flow rate at the end of a length of heating path L, may be written as $(dW/dt)_L$ where,

$$\left(\frac{dW}{dt}\right)_L = \frac{h_m\,(T_s - T_m)\,B\,.\,L}{[\lambda + C_p\,(T_m - T)]}. \qquad (9)$$

Thus, for turbulence to occur, at this point, by combining (8) and (9)

$$\frac{h_m\,(T_s - T_m)\,B\,.\,L}{[\lambda + C_p\,(T_m - T)]} > 1050\,B\mu$$

or

$$L \text{ must exceed } \frac{1050\,\mu\,[\lambda + C_p\,(T_m - T)]}{h_m\,.\,(T_s - T_m)}. \qquad (10)$$

Substituting for h_m from (5),

$$L \text{ must exceed } 18{,}350^{*}\left[\frac{\mu[\lambda + C_p\,(T_m - T)]}{k\,(T_s - T_m)}\right]\left[\frac{\mu^3}{g\,\varrho\,(\sigma + \varrho\cos\theta}\right]^{0{\cdot}33} \qquad (11)$$

(*Substitute 23360 when D_o replaces L).

In all ordinary cases, therefore, the length L is so small comparatively, as to preclude turbulence.

Apparatus

The apparatus consisted of a heating surface—either in the form of a steel platen, or copper tubes—arranged in a sump. The dimensions of the plane surface were varied between 10 cm and 50 cm in both length and breadth. Tubular surfaces were provided as two parallel rows of tubes, arranged on a 60 degree pitch of one outer tube diameter. Tubes with outer diameter of 0·635 cm, 1·270 cm, 2·154 cm, and 5·080 cm were used. The heating surface could be fixed at any angle to the vertical by means of adjustable legs. Insulated side plates could be adjusted to enclose any desired amount of heating surface. The heating surface was fitted with thermocouple junctions.

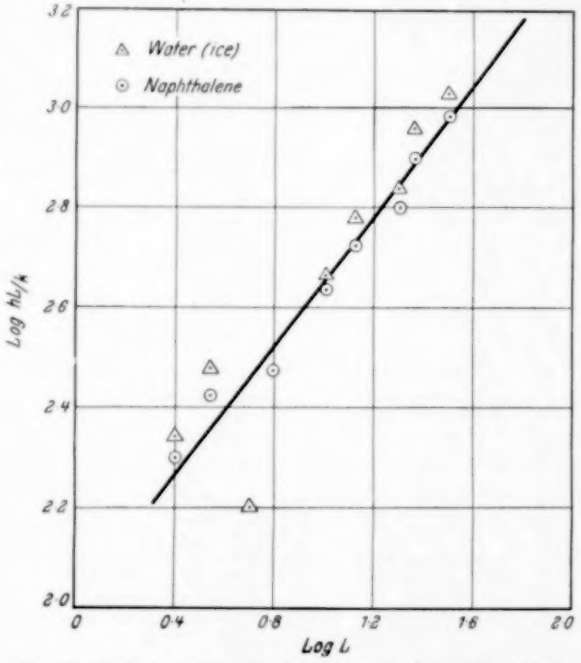

Fig. 1. Effect of length of heating surface upon heat transfer.

Procedure

In an experiment, the heating surface was adjusted to the required angle, with the front edge horizontal. A charge of material, prepared as a solid block or as sized pellets, was added to the apparatus, thermocouples inserted, and weights placed upon it, if it was desired to alter the loading.

Steam was then admitted to the heating surface, and after an initial steadying period, the molten substance was collected and weighed at timed intervals.

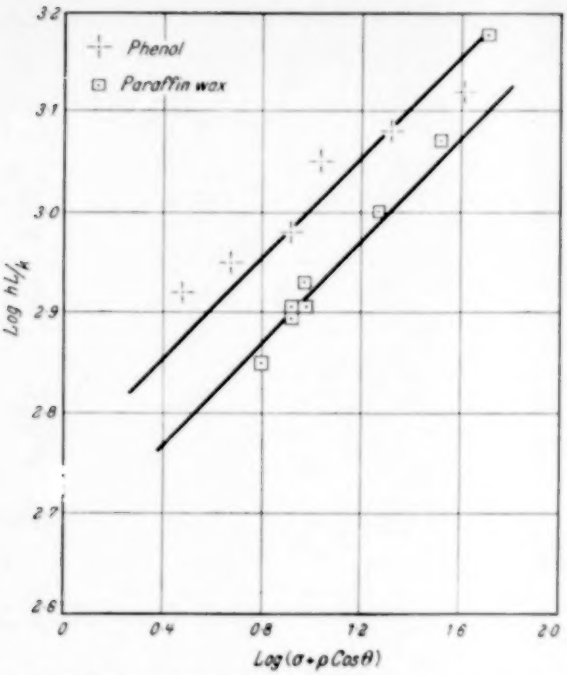

Fig. 2. Effect of loading pressure (σ) and inclination of heating surface (θ) upon heat transfer.

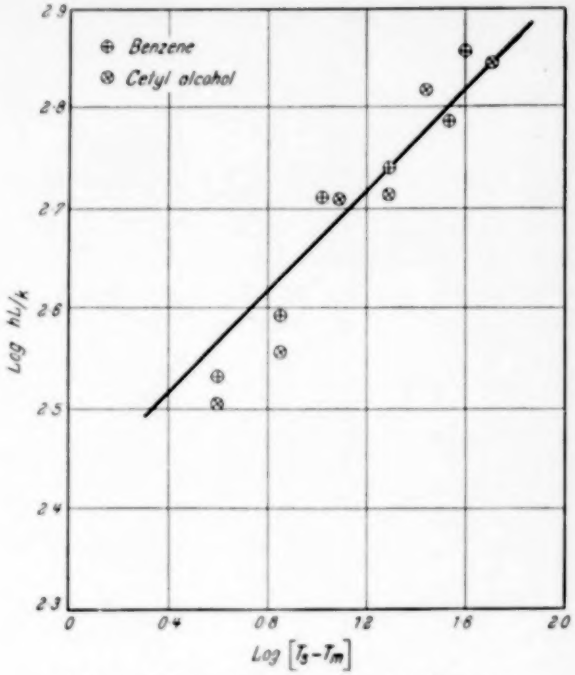

Fig 3. Effect of $T_s - T_m$ upon heat transfer.

VOL. 1 1952

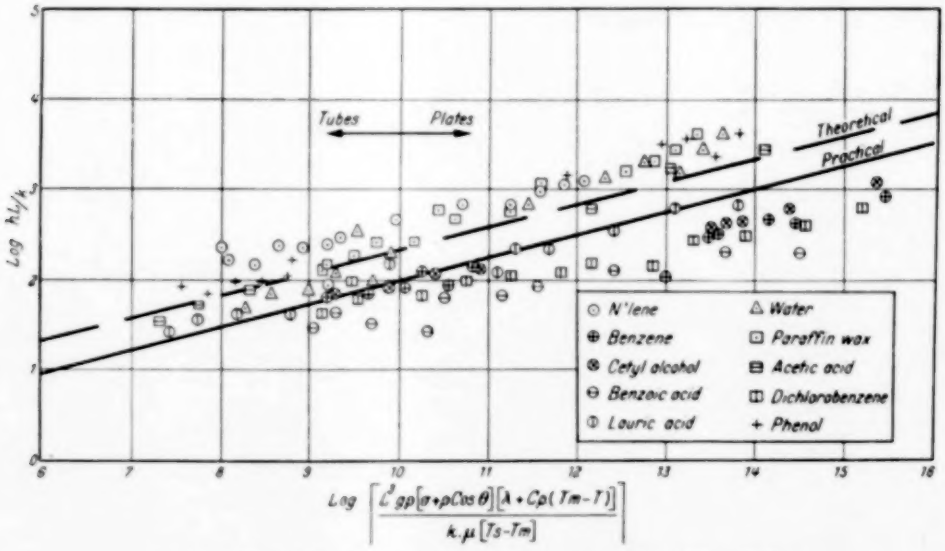

Fig. 4. Correlation of general results, by means of eq. (6) and (7).

Results

Mean heat transfer coefficients were calculated from the observed melting rate, the latent and sensible heats involved, and the temperature difference between the heating surface and the solid.

The physical properties of the molten film were extracted from usual sources [7]. Much of this data was not available at all temperatures, and extrapolation was used.

Eqs. (6) and (7) suggest that the effect of the length of the melting path (L or D_o), the bearing pressure and the draining effects ($\sigma + \varrho \cos \theta$), and the temperature difference ($T_s - T_m$) should be investigated. Some results are presented in Figs. 1, 2 and 3, in which

the full lines represent the slope predicted by eqs. (6) and (7).

These, and other results are plotted in Fig. 4 to show their relationship to the theoretical eqs. (6) or (7),—represented by the broken line.

Although the scatter of individual points is serious, it will be observed that for any single compound the divergence is less wide. It would appear that the unreliable physical data is responsible for this. It is

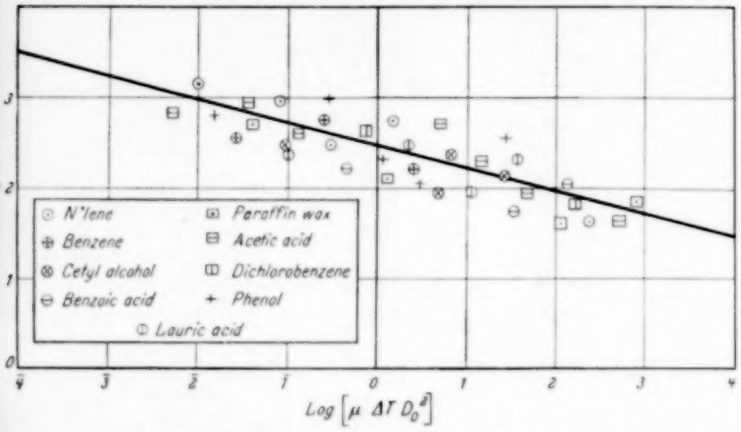

Fig. 5. Comparison of some practical results with the empirical equation.

$$h = \frac{300}{\mu^{0.25}(T_s - T_m)^{0.25} D_o^{0.50}} \, J \sec^{-1} m^{-2} (°C)^{-1}.$$

also of interest to note the degree of agreement between results obtained on tubes, and plane surfaces. It should also be recorded that when the solid material was prepared as pellets, the loading effect was apparently limited to that due to a height of charge of about three times the container side.

The results for granular organic compounds, and tubular surfaces may also be interpreted by a shorter, empirical equation, in which those physical properties which are reasonably similar for different materials are neglected. This formula is

$$h_m = \frac{300}{\mu^{0.25}(T_s - T_m)^{0.25} D_o^{0.5}} \, J \cdot \sec^{-1} \cdot m^{-2} \cdot (°C)^{-1}. \quad (12)$$

The correlation given by this equation may be judged from Fig. 5.

Conclusions

The theoretical equation for heat transfer to a fusible solid may be evaluated from the formulae for plane surfaces,

$$\frac{h_m \cdot L}{k} = 0{\cdot}666 \left[\frac{L^3 g \varrho (\sigma + \varrho \cos\theta)[\lambda + C_p(T_m - T)]}{k \cdot \mu (T_s - T_m)} \right]^{0.25}$$

or,

$$\frac{h_m \cdot D_o}{k} = 0{\cdot}710 \left[\frac{D_o^3 g \varrho (\sigma + \varrho \cos\theta)[\lambda + C_p(T_m - T)]}{k \cdot \mu (T_s - T_m)} \right]^{0.25}$$

for tubes.

The following shorter form of this equation was found to be satisfactory for use with tubes, and granular organic materials.

$$h_m = \frac{300}{\mu^{0.25}(T_s - T_m)^{0.25} \cdot D_o^{0.5}} \, J \cdot \sec^{-1} \cdot m^{-2} \cdot (°C)^{-1}.$$

Notation

A = heating area m²
B = width of heating surface m
C_p = Specific heat of fusible solid $J \cdot kg^{-1} \cdot (°C)^{-1}$
D_o = outer diameter of tube m
g = acceleration due to gravity $m \cdot sec^{-2}$
h = local heat transfer coefficient in molten film $J \cdot sec^{-1} \cdot m^{-2} \cdot (°C)^{-1}$
h_m = mean heat transfer coefficient in molten film $J \cdot sec^{-1} \cdot m^{-2} \cdot (°C)^{-1}$
k = thermal conductivity of molten film $J \cdot sec^{-1} \cdot m^{-1} \cdot (°C)^{-1}$
L = length of plane heating surface m
m = thickness of molten film m
Q = heat J
Re = Reynolds number
t = time sec
T = initial temperature of solid material °C
T_m = melting point of solid material °C
T_s = Temperature of heating surface °C
V = velocity in film $m \cdot sec^{-1}$
W = mass flow in film kg
x = dimension in molten film m
θ = angle of heating surface to vertical
λ = latent heat of fusion $J \cdot kg^{-1}$
μ = viscosity of molten film $kg \cdot m^{-1} \cdot sec^{-1}$
ϱ = density of molten film $kg \cdot m^{-3}$
σ = pressure gradient in film due to weight of solid $kg \cdot m^{-3}$

References

[1] Ingersoll, L. R., Zobel, O. J. and Ingersoll, A. C.; Heat Conduction, McGraw-Hill Book Co. 1948. [2] Pekeris, C. L. and Slichter, L. B.; J. Appl. Physics 1930 **10** 135. [3] Joslyn, M. A. and Marsh, G. L.; Ind. Eng. Chem. 1930 **22** 1192. [4] Hixson, A. W. and Baum, S. J.; Ind. Eng. Chem. 1942 **34** 194. [5] Mitchell, A. G. M. in The Mechanical Properties of Fluids, Blackie & Sons, London 1923. [6] Nusselt, W.; VDI., 1913 **60** 541. [7] International Critical Tables. McGraw-Hill Book Co. 1933. Handbook of Chemistry and Physics (30th Ed. 1941). Chemical Rubber Publishing Co. Timmermans, J.; Physico-Chemical Constants of Pure Organic Compounds. Elsevier 1950.

Quelques problèmes de Génie Chimique concernant la mise au point des procédés catalytiques dans l'industrie des combustibles liquides

Communication présentée au Congrès International de Chimie Industrielle à Paris, Novembre 1951

H. VERSCHOOR, M.Sc.

Bataafsche Petroleum Maatschappij (Groupe *Royal Dutch/Shell*). The Hague, Holland

(Received 25 February 1952)

Résumé—L'auteur donne un aperçu des problèmes technologiques que pose la mise au point des procédés catalytiques, suivant les divers modes operatoires choisis: travail sur lit fixe, travail par percolation, travail sur bouillie, travail sur lit mobile ou sur lit fluidisé.

Les résultats des études fondamentales montrent que celles qui sont relatives au lit fixe sont les plus avancées, mais qu'il nous manque encore beaucoup de données pour les autres modes opératoires.

Summary—A survey is given of some chemical engineering problems occurring in the development and design of catalytic processes. They refer to the various methods for carrying out catalytic reactions, viz. fixed bed, trickle, slurry, moving bed and fluidized bed operation.

The results of fundamental studies show, that so far most data are available for the fixed bed processes but that many more are required particularly when referring to the other methods of operation.

1. INTRODUCTION

Le développement des procédés catalytiques dans l'industrie du pétrole et des carburants synthétiques est très remarquable. C'est aux Etats Unis surtout, qu'on s'est rendu compte de l'importance de la catalyse hétérogène et particulièrement de la catalyse de contact. Ce développement est d'autant plus frappant si nous considérons l'accroissement des procédés pour la fabrication d'essence d'aviation. Par exemple, pour le cracking catalytique, la capacité est passée de 10000 barils par jour en 1936 à 1700000 barils par jour en 1950.

La solution des problèmes qui se sont présentés et qui se présentent toujours dans la réalisation d'un procédé catalytique est seulement possible s'il y a une collaboration incessante entre le chimiste, faisant les recherches fondamentales concernant le catalyseur, et l'ingénieur du génie chimique.

En ce qui concerne les qualités exigées d'un catalyseur industriel, celles-ci ont été décrites largement par HOOG [8] et peuvent être résumées comme suit:

1) Activité: les conditions de réaction doivent être telles que l'équilibre soit le plus favorable.

2) Sélectivité: la composition du catalyseur doit être telle que la réaction qui nous donne le produit désiré soit favorisée.

3) Durée de vie du catalyseur: ceci est de première importance pour l'économie du procédé.

4) Résistance mécanique: ce facteur a une importance spéciale pour les convertisseurs à lit fixe.

Dans cette communication je me propose de vous soumettre un aperçu d'un certain nombre de problèmes de technologie dans la mise au point d'un procédé catalytique, aussi bien dans l'usine pilote qu'à l'échelle industrielle.

2. LA NATURE DES PROBLÈMES ET LES DIFFÉRENTS MODES OPERATOIRES

La nature des problèmes qui peuvent se présenter a conduit à différents modes operatoires pour les réactions catalytiques. La conception des convertisseurs demande en général une connaissance des facteurs suivants, qu'il ne faut surtout pas sous-estimer puisqu'ils déterminent les possibilités du procédé au point de vue économique. Ce sont:

1) les lois hydrodynamiques qui portent sur l'écoulement des fluides et du catalyseur;

2) les lois de transfert de matière entre les fluides et les particules de catalyseur;

3) les lois de transfert de chaleur du catalyseur aux parois du réacteur et vice versa.

A côté de ceux-ci on peut avoir le problème de la régénération du catalyseur, par exemple dans le cas du dépôt sur le catalyseur d'un produit diminuant son activité. Cet effet est très marqué dans le cracking catalytique, où le dépot de coke peut être de l'ordre de 7 g/l. La régénération se fait par brûlage du coke avec de l'air éventuellement dilué avec de l'azote ou de la vapeur d'eau.

Les différentes méthodes pour réaliser des réactions catalytiques à l'échelle industrielle sont résumées dans le tableau suivant et illustrées par un exemple industriel.

Tableau 1. Modes opératoires des procédés catalytiques

Travail sur lit fixe		*Travail sur touillie*	*Travail sur lit mobile*	*Travail sur lit fluidisé*
A. Réaction en phase gazeuse	B. Travail par percolation Système: gaz-liquide Liquide sous forme de Couche mince	Système: gaz-liquide Catalyseur en suspension dans le liquide	Réaction en phase gazeuse	Réaction en phase gazeuse
Exemples	*Exemples*	*Exemples*	*Exemples*	*Exemples*
Hydrogénation des oléfines	—	Hydrogénation des oléfines	—	—
—	—	Hydrogénation du charbon	—	—
Oxydation de l'o-xylène	—	—	—	Oxydation de l'o-xyléne
—	—	Oxydation de paraffines	—	—
Cracking du gasoil	—	—	Cracking du gasoil	Cracking du gasoil
Synthèse des hydrocarbures	Synthèse des hydrocarbures	Synthèse des hydrocarbures	Synthèse des hydrocarbures	Synthèse des hydrocarbures

Nous ne voulons signaler ici que quelques procédés qui peuvent être réalisés de façons différentes. Les exemples comprennent des réactions d'hydrogénation, d'oxydation, de cracking et de synthèse des hydrocarbures.

Dans la section suivante on va examiner les problèmes qui se présentent pour les différents modes opératoires. Quoique les développements récents nous aient donné les procédés sur lit fluidisé et sur lit mobile, c'est surtout le réacteur sur lit fixe qui est toujours le plus utilisé à cause de sa simplicité.

3. Travail sur Lit Fixe

A. Réactions en phase gazeuse

La conception d'un réacteur sur lit fixe n'offre aucun problème sérieux si la réaction a lieu avec un effet thermique peu important. Cependant pour la plupart des réactions catalytiques, l'effet thermique est considérable et l'élaboration du réacteur le mieux adapté demande une étude importante.

Nous n'avons qu'à songer au cracking Houdry, où pendant une période de régénération de 10 minutes dans un réacteur ayant un volume net de catalyseur de 30 m³, la quantité de chaleur développée atteint $1{,}3 \times 10^6$ kcal. C'est surtout ce problème de transfert de quantités de chaleur importantes qui a conduit au développement du catalyseur fluidisé.

Nous pouvons maintenant distinguer les problèmes qui ont trait à l'écoulement des fluides, et ceux concernant la transmission de chaleur et le transfert de matière.

a) *La perte de charge dans un lit fixe*—La perte de charge pour l'écoulement d'un fluide à travers un lit fixe de catalyseur peut être calculée au moyen de la relation existant entre la perte de charge et le facteur de frottement, celui-ci étant une fonction du nombre de Reynolds. Cette relation est analogue à celle pour l'écoulement d'un fluide dans les conduites. D'après Blake [3] et Carman [5] la relation est la suivante:

$$\frac{\Delta p}{\varrho\, v^2} \cdot \frac{1}{S\, l} \cdot \varepsilon^3 = f(Re)$$

où

Δp = perte de charge
ϱ = densité du fluide
v = vélocité linéaire
l = hauteur du lit
S = surface extérieure du catalyseur par unité de volume du réacteur
ε = porosité du lit.

Un aperçu des données pour des catalyseurs de forme différente a été donné par Verschoor [14].

b) *Transfert de chaleur et de matière*—Ce transfert se fait par conduction thermique respectivement par

diffusion et par convection. Suivant les auteurs, c'est tantôt la transmission de chaleur par conduction, tantôt le transfert par convection qui est le plus important dans la transmission de la chaleur aux parois du convertisseur à lit fixe (transport) normal au sens de l'écoulement du fluide). C'est grâce au travail de BAKHUROV et BORESKOV [1] qu'on a appris que le transfert a lieu aussi bien par conduction que par convection. DAMKÖHLER [7] a introduit pour le transfert de chaleur et de matière dans un lit fixe les concepts de conductivité tourbillonnaire (eddy conductivity) et de diffusivité tourbillonnaire (eddy diffusivity), en relation directe avec la vitesse linéaire du fluide v ainsi qu'avec le diamètre du catalyseur d_p suivant:

$$E = C\,v\,d_p$$

où C est une constante sans dimension. E a la dimension d'un coefficient de diffusion ($L^2\ T^{-1}$). Pour le cas analogue de la conduction thermique, E doit être multiplié par $c_p\,\varrho$, où c_p est la chaleur spécifique et ϱ la densité. DAMKÖHLER donne la relation suivante:

$$\lambda_{\text{effectif}} = \lambda_0 + c_p\,\varrho\,C\,v\,d_p$$

où λ_0 est la conduction thermique du lit sans écoulement de fluide.

C'est à KLINKENBERG [10] que nous devons d'avoir montré, en dérivant la valeur de C des différentes recherches expérimentales, qu'il y a une bonne corrélation entre la théorie de DAMKÖHLER et les données de BAKHUROV et BORESKOV, de BERNARD et WILHELM [2] et de COBERLY et MARSHALL [6]:

Auteurs	*Transfert de*	*Fluide*	*Valeur de C*
BAKHUROV et BORESKOV	Chaleur et matière	Gaz	0,16
BERNARD et WILHELM	Matière	Liquide	0,20
COBERLY et MARSHALL . . .	Chaleur	Gaz	0,18

B. Travail par percolation

Dans ce cas, un film d'un liquide traverse le lit de catalyseur, le gaz passant généralement en courant parallèle. Les problèmes, par exemple la distribution du liquide et la teneur en liquide (le «hold-up») de la colonne, sont surtout de nature hydrodynamique et en général analogues à ceux qu'on rencontre dans les colonnes de distillation ou d'absorption avec anneaux RASCHIG. De cette façon on a trouvé que la distribution uniforme du liquide dans le lit de catalyseur s'effectue seulement si le rapport entre le diamètre du réacteur et celui de la particule est superieur à une valeur minimum.

4. TRAVAIL SUR BOUILLIE

Dans ce cas, le gaz traverse en forme de bulles une couche de liquide dans laquelle le catalyseur pulvérulent se trouve en suspension. L'application de cette opération pose surtout des problèmes hydrodynamiques comme la distribution des bulles de gaz dans la colonne de liquide et la formation des bulles ainsi que leur grandeur. Une étude préliminaire de VERSCHOOR [15] a montré que la teneur en gaz d'un tel système gaz-liquide augmente avec le débit de gaz jusqu'à un point critique, à partir duquel la teneur en gaz diminue pour augmenter de nouveau quand on continue à augmenter le débit de gaz. Une courbe donnant la relation entre la vitesse ascendante des bulles de gaz et la teneur en gaz du système montre qu'on peut distinguer trois régions en augmentant le débit du gaz: d'abord, une région dans laquelle la teneur en gaz augmente tandis que la vitesse ascendante des bulles reste plus ou moins constante, ensuite une région où la teneur en gaz reste plus ou moins constante tandis que la vitesse des bulles croît; finalement une région dans laquelle l'une et l'autre augmentent simultanément.

5. TRAVAIL SUR LIT MOBILE

Dans les convertisseurs sur lit mobile on a un ensemble de particules ayant un contact direct entre elles et gardant approximativement une position fixe les unes par rapport aux autres, l'ensemble étant en mouvement par rapport aux parois du réacteur. Quoique pour ce mode opératoire on puisse s'attendre à rencontrer également des problèmes hydrodynamiques et de transmission de chaleur, jusqu'à présent très peu a été publié à ce sujet dans la littérature. En ce qui concerne la perte de charge dans un lit mobile nous pouvons nous référer à une communication de NEWTON, DUNHAM et SIMPSON [12].

6. TRAVAIL SUR LIT FLUIDISÉ

Un aperçu général des phénomènes caractéristiques d'un lit de catalyseur fluidisé a été donné par KALBACH [9] et par WILHELM [18], qui considèrent spécialement l'état de fluidisation dense. La plupart des études publiées traitent surtout de la perte de charge

VOL. 1 1952

dans le lit fluidisé dense: pour la fluidisation aggrégative (WILHELM et KWAUK [19], LEVA et collaborateurs [11]) et pour la fluidisation particulaire (WILHELM et KWAUK [19], BRINKMAN [4], VERSCHOOR [16]). C'est surtout pour cette dernière forme de fluidisation, qui se fait à l'aide d'un liquide, que le caractère de la relation entre la vitesse linéaire du liquide et la hauteur du lit dilaté, donc la porosité correspondante, est établi. Si un lit de catalyseur est en état de fluidisation particulaire, la porosité de la phase dense est uniforme. D'autre part, dans un lit en état de fluidisation aggrégative, on peut observer des bulles d'une grande porosité traversant un système d'une porosité inférieure. Le système présente alors l'image d'un liquide bouillant. Cette dernière forme est observée surtout si la fluidisation est faite à l'aide d'un gaz, et elle est caractéristique pour les lits fluidisés à l'échelle industrielle. A cause du brassage intense le contenu d'un réacteur sur lit fluidisé est presque homogène, et par conséquent la transmission de chaleur du système aux parois du convertisseur est très élevée de sorte que les gradients de température, qu'on signale souvent dans les convertisseurs sur lit fixe, ne se montrent pas dans les lits fluidisés.

Au sujet des études de transfert de matière, très peu a été publié, tandis que pour la transmission de chaleur, VREEDENBERG [17] a donné un aperçu de ses résultats ainsi que de ceux d'autres auteurs. VREEDENBERG trouve des coefficients de transmission de chaleur variant de 95 kcal/m². °C.h. jusqu'à 450 kcal/m². °C.h. selon les conditions de l'écoulement.

Finalement il faut signaler la communication importante de REIS [13] qui, ayant rappelé les résultats des études pour le lit fluidisé dense, a présenté une étude sur le lit fluidisé léger, c'est à dire l'état d'une suspension dispersée.

7. CONCLUSION

Nous avons passé en revue un nombre important de problèmes de Génie Chimique qui se posent dans la mise au point des procédés catalytiques. Il apparait qu'en ce qui concerne les problemes d'écoulement des fluides, de transfert de chaleur et de matiére, nous soyions en mesure de calculer un convertisseur à lit fixe. Il n'en est pas de même pour les autres types de convertisseurs et il nous reste encore de nombreux problèmes dont la solution demandera d'autres études approfondies.

NOTATION

Δp = perte de charge
ϱ = densité de fluide
v = vélocité linéaire
l = hauteur du lit
S = surface extérieure du catalyseur par unité de volume du réacteur
ε = porosité du lit
C = constante sans dimension
E = eddy conductivity ou eddy diffusivity
d_p = diamètre du catalyseur
λ = coefficient de conduction thermique
c_p = chaleur spécifique

BIBLIOGRAPHIE

[1] BAKHUROV, V. G. et BORESKOV, G. K.; La conduction thermique effective des lits de catalyseur. J. Appl. Chem. (USSR) 1947 **20** (Nr 8). [2] BERNARD, R. A. et WILHELM, R. H.; Diffusion turbulente dans les lits fixes de catalyseur. Chem. Eng. Progr. 1950 **46** 233. [3] BLAKE, F.C.; La perte de charge d'un fluide traversant un lit de particules. Trans. Amer. Inst. Chem. Engrs 1922 **14** 415. [4] BRINKMAN, H. C.; Calcul de la force visqueuse excercée par un fluide en mouvement sur un ensemble dense de particules. Appl. Sci. Res. 1949 **A1** 27. [5] CARMAN, P. C.; L'écoulement d'un fluide à travers un lit de particules. Trans Inst. Chem. Engrs (Lond.) 1937 **15** 150. [6] COBERLY, C. A. et MARSHALL, W. R.; Gradients de température dans un courant de gaz traversant un lit fixe de particules. Chem. Eng. Progr. 1951 **47** 141. [7] DAMKÖHLER, G.; Voir Eucken et Jakob, Der Chemie Ingenieur, Bd. III, Teil 1. Akad. Verlagsgesell., Leipzig 1938. [8] HOOG, H.; Choix et développement de catalyseurs dans l'industrie chimique. Conf. à la «Society of Chemical Industry» Londres, 12 déc. 1950. [9] KALBACH, J. C.; La fluidisation appliquée dans des réactions chimiques. Chem. Eng. 1947 **54** (janvier) 105. [10] KLINKENBERG, A.; Choix de réacteurs catalytiques. Chem. Weekbl. 1950 **47** 472. [11] LEVA, M. *et coll.*; Introduction sur la fluidisation. Chem. Eng. Progr. 1948 **44** 511, 619, 707. [12] NEWTON, R. H., DUNHAM, G. S. et SIMPSON, T. F.; Le procédé TCC pour fabrication d'essence moteur. Trans. Amer. Inst. Chem. Engrs 1945 **41** 215. [13] REIS, T.; Contribution à l'étude théorique et expérimentale des systèmes à catalyseurs fluidisés. Bulletin A.F.T.P. 1949, Nr 76, août. [14] VERSCHOOR, H.; La perte de charge pour l'écoulement des fluides à travers un lit fixe de catalyseur. De Ingenieur 1950 **62** Ch. 5. (en anglais). [15] VERSCHOOR, H.; Quelques aspects du mouvement d'un groupe de bulles de gaz à travers une colonne liquide verticale. Trans. Inst. Chem. Engrs (Lond.) 1950 **28** 52. [16] VERSCHOOR, H.; Données expérimentales sur la force visqueuse exercée par un fluide en mouvement sur un ensemble dense de particules. Appl. Sci. Res. 1950 **A2** 155. [17] VREEDENBERG, H. A.; Transmission de chaleur dans un lit fluidisé. Communication pour le congrès de «Heat Transfer» organisé par le «Institution of Mechanical Engineers» à Londres, Sept. 1951. [18] WILHELM, R. H.; La fluidisation des particules. Research 1950 **3** 159. [19] WILHELM, R. H. et KWAUK, M.; Fluidisation des particules solides. Chem Eng. Progr. 1948 **44** 201.

Heat transfer to air flowing through heated tubes

Part I: Effect of entry and exit conditions
Part II: Effect of length to diameter ratio

Y. C. Chu and J. Anderson Storrow

Chemical Engineering Laboratory, College of Technology, Manchester, England

(Received 6 December 1951)

Summary. *Part I*—A preliminary study has been made of the effect of various end conditions on surface conductances to air flowing through a heated tube.

The effects of thermometric errors and flow disturbances lead to characteristic forms for the variation of surface conductance with flow characteristics. The inlet disturbance produced large changes from the accepted correlation forms for nominally streamline flow for values of Graetz number between 5 and 300 in tubes with lengths 12 to 48 times their diameters.

Part II—Surface conductances have been measured in the transfer of heat from the wall of a steam heated tube to air flowing through the tube of 1 in. diameter, the flow being disturbed at the inlet by a perforated plate and gauze. A range of L/D_t of 4:1 has been tested. Three regions of flow have been observed in the range of Re from (a) 100 to 250 $(L/D_t)^{0.16}$, (b) 250 $(L/D_t)^{0.16}$ to 2200, (c) 2200 to 4000. The surface conductances for region (b) agree with the equation

$$Nu = 0{\cdot}76\left(\frac{L}{D_t}\right)^{-0.75}(Re)^{0.70}.$$

In the flow range wherein $D_tG/\mu < 2200$ the following equations apply:

$$Nu = 0{\cdot}95\,(Gr)^{0.70} \quad \text{for} \quad (Gr) > 5{\cdot}8$$

$$Nu = 0{\cdot}55\,(Gr) \quad \text{for} \quad (Gr) < 5{\cdot}8.$$

Résumé—*Première partie.* Etude préliminaire de l'influence de différentes conditions terminales sur le coefficient spécifique de transmission thermique d'une surface vis-à-vis d'air s'écoulant dans un tube chauffé.

Les effets des erreurs thermométriques et des perturbations dans l'écoulement conduisent à des formes caractéristiques pour la variation de la conductance avec les caractéristiques de l'écoulement. La perturbation d'entrée introduit des écarts considérables avec les corrélations usuellement acceptées pour des écoulements laminaires (nombre de Graetz compris entre 5 et 300, tubes dont les longueurs varient entre 12 et 48 diamètres).

Deuxième partie. Mesures de conductances de surface dans l'échange thermique entre la paroi chauffée à la vapeur et l'air traversant un tube de 25 mm diam. A l'entrée, l'écoulement est modifié par une plaque perforée et une toile. Les expériences ont couvert une gamme de 4 à Fig. 1 pour L/D_t et trois régimes d'écoulement avec Re compris entre:

(a) 100 et 250 $(L/D_t)^{0.16}$
(b) 250 $(L/D_t)^{0.16}$ et 2200
(c) 2200 et 4000

Pour le régime (b), les résultats sont bien représentés par:

$$Nu = 0{,}76\,(L/D_t)^{-0{,}75}(Re^0)^{0{,}70}$$

tandis qu'avec $D_tG/\mu < 2200$, les réactions deviennent:

$$Nu = 0{,}95\,(Gr)^{0{,}70} \quad \text{pour} \quad (Gr) > 5{,}8$$

$$Nu = 0{,}55\,(Gr) \quad \text{pour} \quad (Gr) < 5{,}8.$$

Part I. Effect of entry and exit conditions

During work on the heat transfer from a heated tube to air flowing through the tube [4], it was observed that slight modifications of the inlet and outlet design caused appreciable differences in the results obtained from the terminal temperature measurements. A variety of simple inlet and outlet devices were tested on a short heating tube, since the average conductances for long tubes are less sensitive to inlet conditions, in order to form an opinion on the importance of these points.

The apparatus used is shown in Fig. 1. Steam under a slight gauge-pressure was supplied to the annular jacket. The steam temperature together with the inlet and outlet temperatures of the air stream were measured with thermometers. The air flow was measured with capillary flowmeters, which had been calibrated against standard meters and the results charted according to the method of Whitwell [12]. The inner tube was fitted with a perforated plate covered with copper gauze of about

VOL. 1 1952

60 mesh to provide a support for packings such as lead shot, glass beads etc., when testing the effect of such packing on the heat transfer from the tube wall to the gas. The heat transfer rates were estimated from the flow rate and bulk temperature rise of the air stream passing through the tube. The surface conductance for heat transfer from the wall to the air was assumed to be equal to the overall coefficient from steam to air considering the

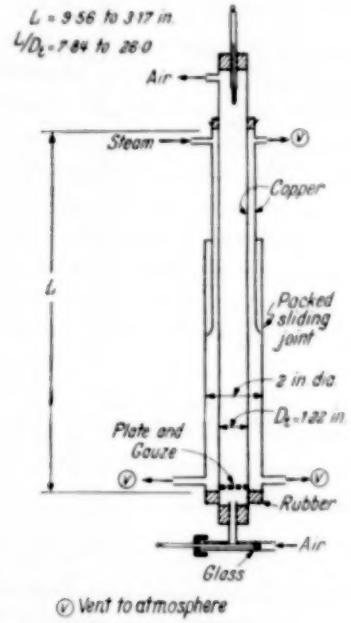

Fig. 1. Simplest heat transfer tube arrangement.

steam condensate film and copper wall as offering negligible resistance to heat transfer compared with the resistance of the air film side. The area for heat transfer was taken to be the heated length of the steam jacket. The jacket consisted of a telescopic tube arrangement which was varied in length to suit the various inner-tube lengths. The heated length was varied from 31·7 to 9·56 in. giving a L/D_t ratio from 26·0 to 7·84.

The following discussion of the effects of inlet and outlet fittings is based mainly on tests of the $L/D_t = 7{\cdot}84$ tube.

Experimental Results

The effect of the inlet and outlet designs shown in Fig. 2, 3, respectively were studied. The data obtained are shown in Fig. 4, 5, 6, and the key to the arrangements is given in Table 1. The experimental results have been based on the arithmetic

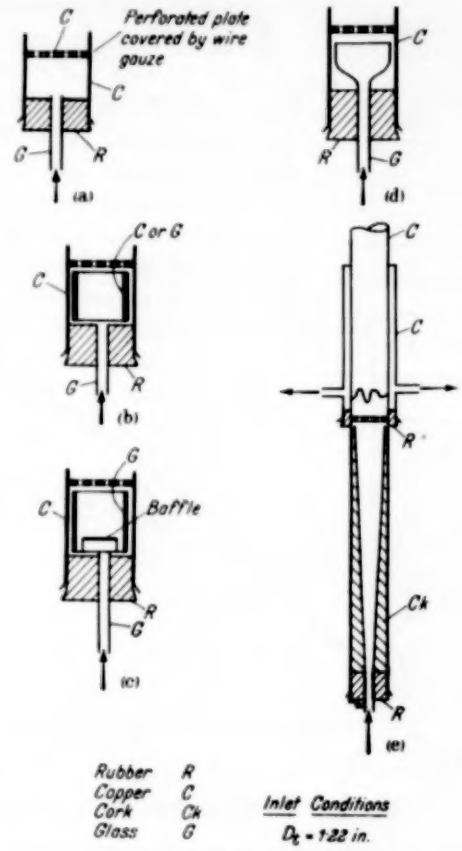

Fig. 2. Inlet arrangements.

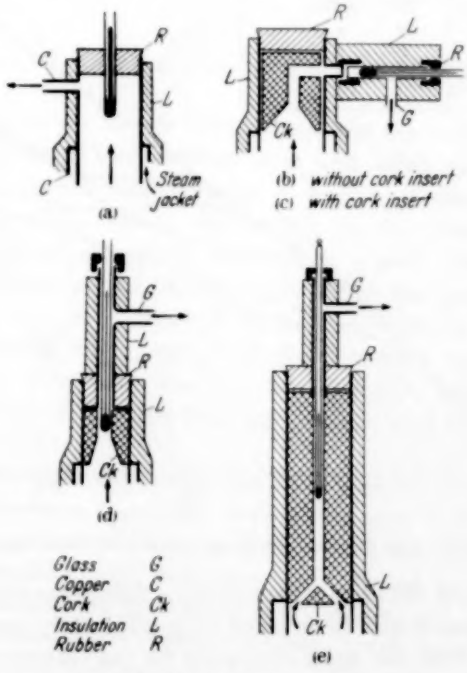

Fig. 3. Outlet arrangements.

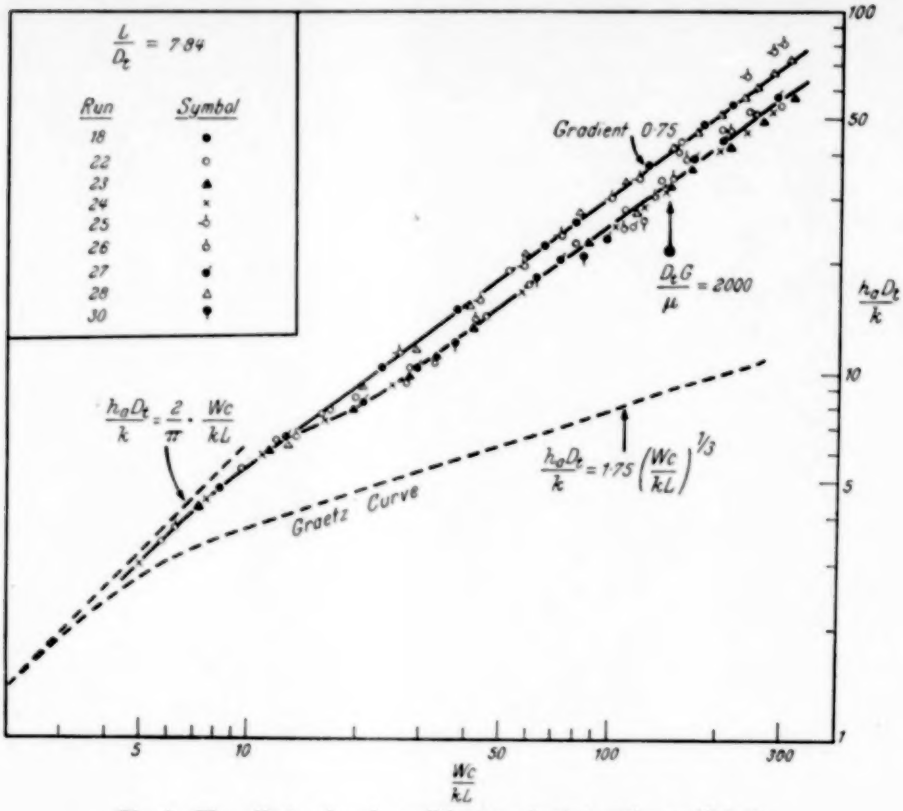

Fig. 4. The effects of end conditions on heat transfer coefficients.

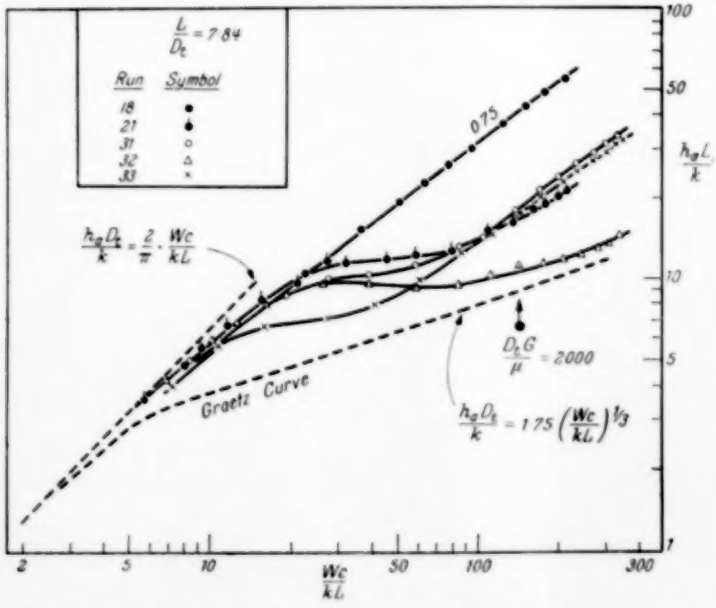

Fig. 5. The effects of end conditions on heat transfer coefficients.

Table 1. Arrangement of inlet and outlet fittings for $L/D_t = 7{\cdot}84$

Figure	Run	Inlet (see Fig. 2)	Outlet (see Fig. 3)	Perforated plate +with −without
4	18	a	a	+
4	22	b	d	+
4	23	b	d	+
4	24	b	d	+
4	25	d	c	+
4	26	d	d	+
4	27	d	d	+
4	28	d	d	−
4	30	c	d	−
5	21	c	d	+
5	31	c	d	+
5	32	c	d	+
5	33	c	d	−
6	20	c	b	+
6	35	c	c	+

mean of the terminal temperature differences between the steam and air in order to provide ready comparison with the usual expression for the GRAETZ function and its associated equations. The GRAETZ equation for heat transfer to a stream having parabolic velocity distribution is given [9] as

$$\frac{h_a D_t}{k} = \frac{2}{\pi}\left(\frac{Wc}{kL}\right)\left(\frac{1-8\varphi(n)}{1+8\varphi(n)}\right) \qquad (1)$$

VOL. 1 1952

where $\varphi(n) = 0{\cdot}10238e^{-14{\cdot}6272n} + 0{\cdot}01220e^{-89{\cdot}22n} + 0{\cdot}00237e^{-212n} + \cdots$

$$n = \frac{\pi}{4}\left(\frac{kL}{Wc}\right).$$

This form is shown in Fig. 4, 5, 6, together with the approximations

$$Nu = \frac{2}{\pi}(Gr) \qquad (2)$$

for Gr values up to about 3, and

$$Nu = 1{\cdot}75\,(Gr)^{\frac{1}{3}} \qquad (3)$$

for $Gr > 10$, up to the limit of streamline flow in a particular tube. The tube of $L/D_t = 7{\cdot}84$ would give a Reynolds number of about 2000 near $Gr = 150$, and the data at higher flow rates corresponding to the higher Gr values would be expected to show evidence of the beginning of transitional flow before attaining full turbulence at perhaps $Re > 10000$. The disturbance of the inlet flow pattern caused by perforated plates, flow direction changes, expansions of cross-section to flow etc., is expected to affect the surface conductance functions mainly in the transition range from the relatively undisturbed laminar motion at very low Gr up to the fully turbulent condition at high Re.

The data have been grouped in Fig. 4, 5, 6 using the data from Run 18 as the common curve as a guide to comparisons.

The data for Run 32 in Fig. 5 fall considerably lower in ordinate than the others, approaching the GRAETZ curve more nearly than any other arrangement. The approach to the GRAETZ curve is probably fortuitous rather than by the production of parabolic velocity distribution and thus conforming to the basic flow regime used in the GRAETZ analysis. The data in Fig. 6 give curves similar to that observed by CHOLETTE [3].

Discussion of Results

In all the experiments in Part I and Part II the heat transfer length was less than that probably required for the decay of eddies caused by the grid support and the establishment of the velocity distribution appropriate to the stable flow regime. Though studies have been made of the decay of turbulence induced by grids [6], [7] and of the development of parabolic velocity distribution from rod flow [2], [10], [11], solutions for the combined problems are not available. The above generalisation seems appropriate in view of the development of parabolic velocity distribution for laminar flow probably requiring [2] a transition length of $0{\cdot}13\,D_t\,.\,Re$ The decay of turbulence may take a length equivalent to a few hundreds of grid-mesh widths [6]. This decay is also sensitive to the turbulence level at the inlet to the grid, which has been observed here and elsewhere [1] in the effect of inlet sections.

The curves in Fig. 4, 5, 6 all agree with the GRAETZ function at low rates, $Gr < 3$, where the

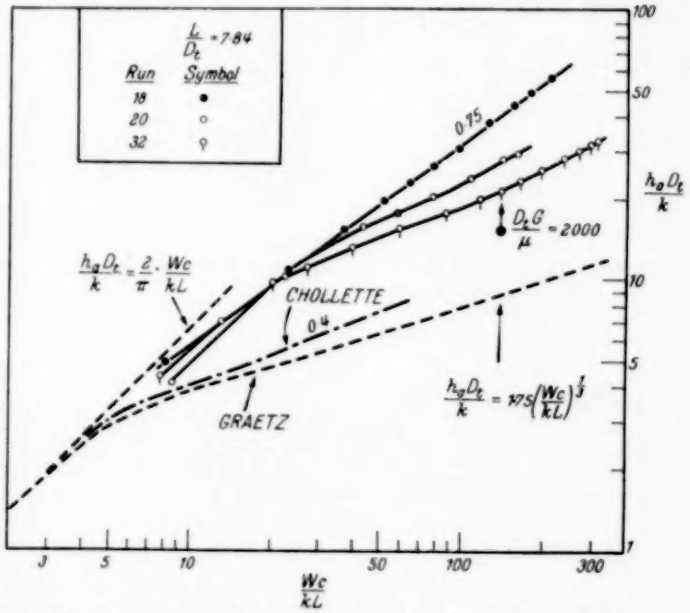

Fig. 6. The effects of end conditions on heat transfer coefficients.

disturbances due to inlet fittings and errors due to radiation to thermometers have little effect and the heat transfer system gives a surface conductance relationship near to the limiting eq. (2). With Gr increasing the curve extends to higher ordinate than that on the GRAETZ curve before the gradient falls to a value, which in many cases could be considered as 0·4, agreeing with the CHOLETTE type of curve. Thereafter the curve changes to a gradient of 0·7 to 0·8 for the flow region up to and beyond $Re = 2000$.

The experiments were not undertaken as a study of turbulence promoters. Two points were at issue: how much the surface conductance and the form of its variation with flow rate were affected by the differences between simple inlet devices, and how far the results were subject to thermometric radiation errors with various outlet designs. The major study

was to be made on packed tubes and thus the designs tested here were only considered qualitatively rather than with any intention of quantitative correlation or description of either the turbulence promotion or the thermometric corrections. The form of the curves for Nusselt number, $\frac{h_a D_t}{k}$, against the group $\frac{Wc}{kL}$ were of interest for comparisons between the data for packed tubes and for empty tubes with disturbed inlet conditions. The variations in the outlet were mainly to reduce radiation errors at the outlet thermometer, which could give estimated errors up to 12% in Nu for the outlet "a" on Fig. 3 and this error would be similar in packed and empty tubes.

The curve for Run 18, used as a "datum" for comparison, was provided by the simplest inlet (a) and outlet conditions (a). The combination of inlet "d" and outlet "c" (Run 25) had no effect on the curve. The inlets "b" and "d" were similar and with outlet "d" gave the lower curve on Fig. 4 (Runs 22–27). The omission of the perforated plate and gauze cover moved the curve from the lower (Run 27) to the upper position (Run 28), when using the inlet "d" and outlet "d". A similar but greater effect is noted on comparing the Run 30 (Fig. 4) with Runs 21, 31 (Fig. 5), wherein the former was without the perforated plate, the inlet "c" being used with outlet "d". The plate reduced the effect of the disturbance initiated by the baffle in the inlet "c". The glass cylinders used in inlets "b", "c" and "d" were expected to reduce the heat transfer to the air from the metal wall below the perforated plate. The data for Runs 25, 26 show the effect of including insulation in the head of the tube to reduce transfer to air from the wall outside the nominal heating length. The effect is small but not negligible.

The use of the expanding inlet "e", seven diameters in length, below the perforated plate had a pronounced effect, shown by comparing Runs 31, 32 on Fig. 5. The omission of the perforated plate made Run 33 data differ considerably from the results of Run 32. As with Runs 30, 21 the removal of the perforated plate lowered the flow rate at which the transfer coefficient curve passed to a gradient of about 0·75. The major difference between the curves for Runs 18, 33 was due to the reduction of the "jet" caused by the small tube in inlet "a", and this effect was still further removed by the insertion of the perforated plate beyond the expanding inlet section.

The curve on Fig. 6 for Run 20 (inlet "c", outlet "b") shows a difference from that for Runs 21, 31 on Fig. 5 which had an outlet "d". This difference is mainly due to the greater radiation error in outlet "d", despite the fact that both designs have high air velocities round the thermometers. Reduced radiation to the thermometers was best obtained by using the outlet "e" which insulated the thermometer bulb surroundings from the hot metal surfaces, provided high air velocity round the bulb, and also reduced the heat transfer from metal wall to air at any position higher than the limit of the nominal heated length at the head of the steam jacket.

The inlet "e" and outlet "e" were adopted for further studies. It is not possible to discuss at length the effects of each of the combinations listed in Table 1, but each variant had a particular point in mind, *e.g.* diverting the air "jet" at the inlet, reducing transfer from metal walls outside the nominal heating length, reducing radiation to thermometers measuring air temperatures.

In comparing data from packed and empty tubes it will be necessary to assess the latter which are likely to be used as a "datum" variation. The opinion that heat transfer in packed tubes is greater than in the empty tube depends on the flow region and the degree of disturbance at the empty tube inlet. At $Gr < 3$ it is very unlikely that the introduction of packing has any appreciable effect. If the inlet conditions are similar to those in Run 18, the effect of packing may be small over a very wide flow range.

Another source of error not mentioned above lies in the possibility of radiation to the inlet thermometer. The above arrangements do not suffer from this defect, the radiation to the thermometer stem being small and the air velocity around the bulb being high. That the error can be high, even when the radiating surfaces are at temperatures less than 200° F, is demonstrated readily by inserting the thermometer at the inlet so that the bulb is near the perforated plate. Fig. 7 includes data for Run 3a on a tube packed with lead shot with inlet "a" and outlet "a", and for Run 3b when the inlet thermometer was placed near the plate. The inlet temperature in Run 3b fell from 73 to 43° C as the flow rate G was increased from 14 to 540 lb/sq ft hr. The inlet air temperature was 17 to 22° C in all the tests. This great error in the measurement of the air temperature is, however, less important than

VOL. 1 1952

would appear at first sight. It affects both the estimation of heat transferred from the air flow rate and temperature rise, and the measurement of the mean temperature difference between the heated wall and the air. The effect on the final plots is exemplified by the lines in Fig. 7 which also includes

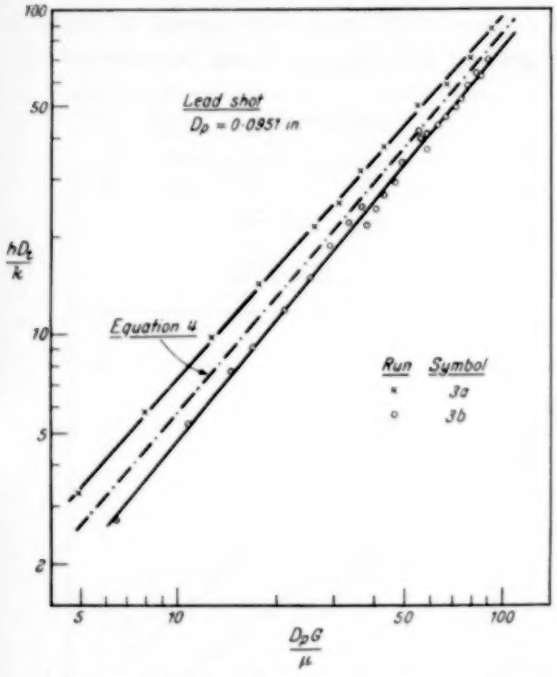

Fig. 7. The effect of thermometric error at the inlet of a packed bed.

a correlation equation proposed elsewhere [5]

$$\frac{h\,D_t}{k} = 0{\cdot}134\left(\frac{L}{D_t}\right)^{-0{\cdot}9}\left(\frac{D_p}{D_t}\right)^{-1{\cdot}13}\left(\frac{D_pG}{\mu}\right)^{1{\cdot}17}. \qquad (4)$$

The data in Fig. 4 are based on the logarithmic mean of the terminal temperature differences between the heated wall and the air stream. The eq. (4) was obtained with an inlet of type "e" and an outlet of type "e". In Fig. 8 examples are given of data from Leva [8] for tubes packed with glass beads, and with lead shot. The data are for downward flow of air through the packing. The inlet thermometer in Leva's apparatus was stated to have been placed close to the packing and appears to have had no radiation shield. The radiation error in Run 3b reduced the ordinates on Fig. 7 by about 30% of the higher value. This may be the main

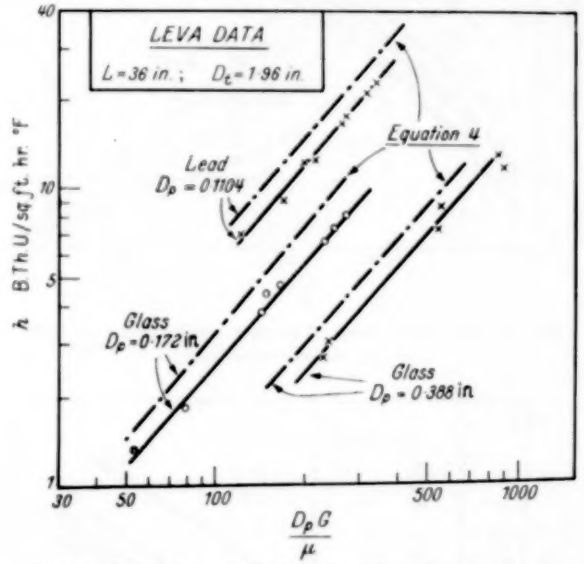

Fig. 8. Comparison with Leva's data for packed beds.

reason why Leva's data in Fig. 8 fall below the correlation found in this laboratory using more shielded thermometers. The discrepancy is also independent of packing conductivity. The Leva outlet temperatures were also stated to have been measured by a thermometer close to the perforated plate support, and these measurements also may have been in error.

Part II. Effect of length to diameter ratio

The following experiments were undertaken to check the high power of mass flow rate associated with surface conductance found in earlier tests on a short tube with disturbed inlet [1] in the flow region below $Re = 2000$, wherein the flow is nominally streamline. The effect of L/D_t ratio was tested using the tube lengths prepared for the associated work on packed beds [5]. It was expected that the ratio would have an effect on the deviation of the heat transfer relation from the eq. (3) for streamline flow when $Gr > 10$.

Experimental Technique

The apparatus used has been described [5], and used the inlet section "e" (Fig. 2) and outlet section "e" (Fig. 3). A thin copper tube of 1 in. diameter was heated by condensing steam. The overall transmission coefficient from steam to air was again assumed to be the surface conductance from the tube wall to the air flowing through the tube. The heat transfer rate was measured by the mass flow rate and terminal bulk temperatures of the air. The surface conductance has been based on the arithmetic mean tem-

perature difference between the tube wall and the air. The physical properties of the air were assessed

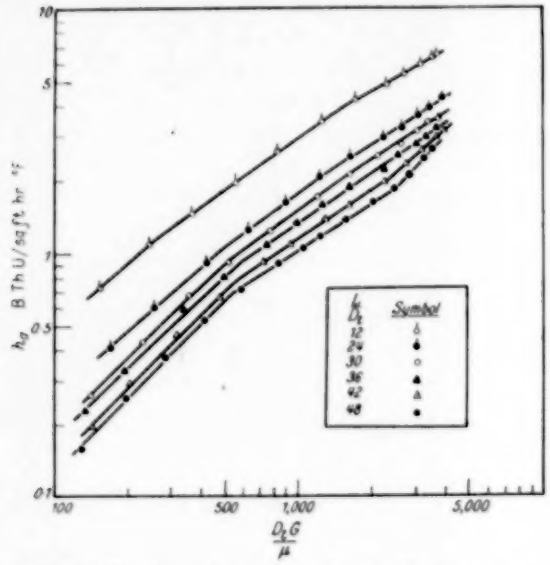

Fig. 9. The dependence of surface conductance on flow rate for various tube lengths.

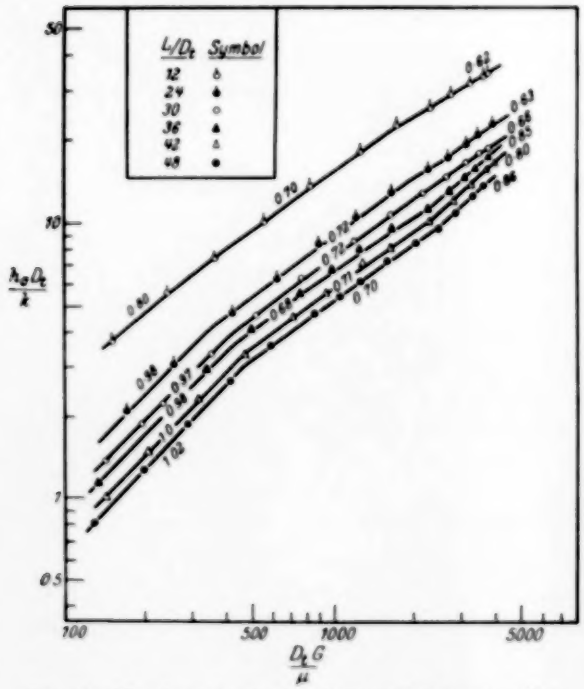

Fig. 10. The dependence of surface conductance on flow rate for various tube lengths.

at the mean air temperature along the tube. The various lengths of heating surface were obtained by cutting the tube and its jacket, and re-making the tube outlet head [5].

Experimental Results

Within the limited experimental range the data on Fig. 9, 10 show three regions wherein the transfer coefficient may be expressed as a power function of mass flow rate, or of $\frac{D_t G}{\mu}$.

The region at $Re > 2200$ contains converging lines for different L/D_t ratios which appear to approach the gradient 0·8 commonly found in turbulent flow

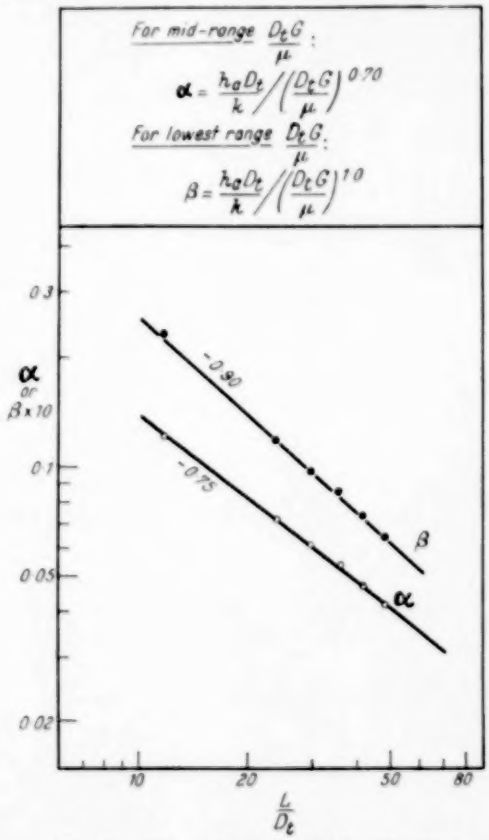

Fig. 11. The analysis of the length effect.

studies. In this intermediate region, preceding the establishment of fully turbulent motion at perhaps about $Re = 10000$, the converging lines suggest that the effect of the L/D_t ratio may become less significant in the turbulent region.

The lines for different L/D_t ratios are parallel at $Re < 2200$. The break point between the region of gradient 0·7 and that of gradient near 1·0 is a function of the Reynolds number. From a logarithmic plot of the critical values, Re_c, it was found that the limit may be expressed as

$$Re_c = 250\left(\frac{L}{D_t}\right)^{0.16}. \qquad (5)$$

VOL. 1 1952

The region from $Re = 250\ (L/D_t)^{0.16}$ up to 2200 contains lines of gradient very near to 0·70, and having a pronounced L/D_t function. The correlation equation for the data may be found by plotting $Nu/Re^{0.7}$ against L/D_t logarithmically as in Fig. 11. The data are correlated by the equation

$$Nu = 0{\cdot}76\left(\frac{L}{D_t}\right)^{-0.75}(Re)^{0.70}. \qquad (6)$$

gradient −0·9 from Fig. 11 the correlation becomes

$$Nu = 0{\cdot}205\left(\frac{L}{D_t}\right)^{-0.9}(Re)^{1.0}. \qquad (7)$$

Since the data for low L/D_t ratios show a considerably lower power for Reynolds number the use of the eq. (7) may be too limited. In view of the approximate equality of powers for (L/D_t) and Re a satis-

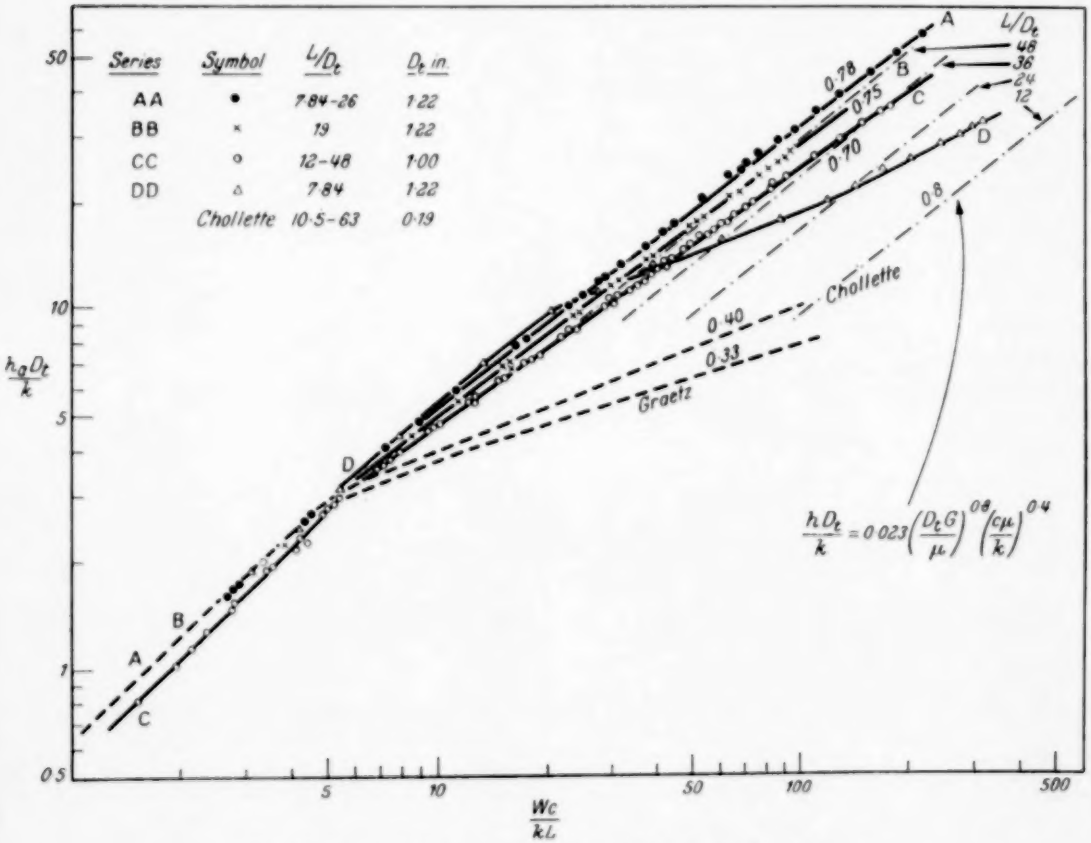

Fig. 12. Comparison with correlations for fully developed flows.

This equation includes the tube diameter in the conventional arguments but its effect as an independent variable has not been tested. It is to be expected that this equation will be limited in application to systems with the high degree of disturbance at the inlet similar to that induced by the present plate and gauze fitting.

The data in the region of lowest flow rates show straight lines whose gradients increase with increasing L/D_t ratio, though this increase is more pronounced with the low ratios. For ratios between 24 and 48 the gradient could be taken as 1·0 and an equation deduced similarly to eq. (6). Accepting the factory correlation is to be expected by incorporating the tube length in Gr. The data plotted as CC in Fig. 12 correlate satisfactorily on one line for all tube lengths over the whole experimental range. For $Gr > 5{\cdot}8$ the line has a gradient 0·70 corresponding to the region in Fig. 9, 10 between $Re = 250\ (L/D_t)^{0.16}$ and $Re = 2200$. The data for $Gr > 5{\cdot}8$ lie on a curve which tends with decreasing flow rate to become parallel to the eq. (2), though giving lower values of Nu at a specific Gr. The eq. (2) is the limiting form for low flow rates of the Graetz function for a parabolic velocity distribution in the tube, given above as eq. (1) and shown in Fig. 12.

From the two straight lines CC on Fig. 12, correlation equations can be obtained. The data for $Gr > 5{\cdot}8$ up to $Re = 2200$ agree with the equation

$$Nu = 0{\cdot}95\,(Gr)^{0{\cdot}70}\,. \tag{8}$$

The data for $Gr < 5{\cdot}8$ agree with

$$Nu = 0{\cdot}55\,(Gr)\,. \tag{9}$$

Discussion of results

The surface conductances measured were the average values for the tube surface from the entrance up to the stated L/D_t value. Fig. 13 contains the data plotted as h_a/cG against Re for each L/D_t ratio, together with an example from Cholette's results [3]

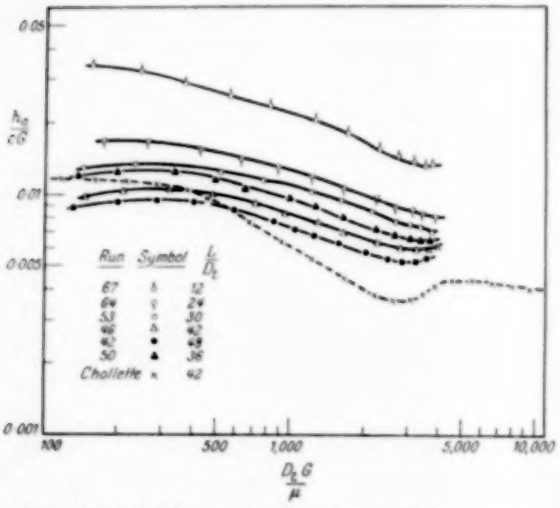

Fig. 13. The effect of length on mean surface conductances.

On the plot of Nu against Gr on Fig. 12, both the Cholette data and the present data show a rapid change of gradient around $Gr = 5$. The results above this value of abscissa correspond to a line of gradient 0·7 whereas the Cholette line has a gradient of 0·4. A discrepancy has been noticed

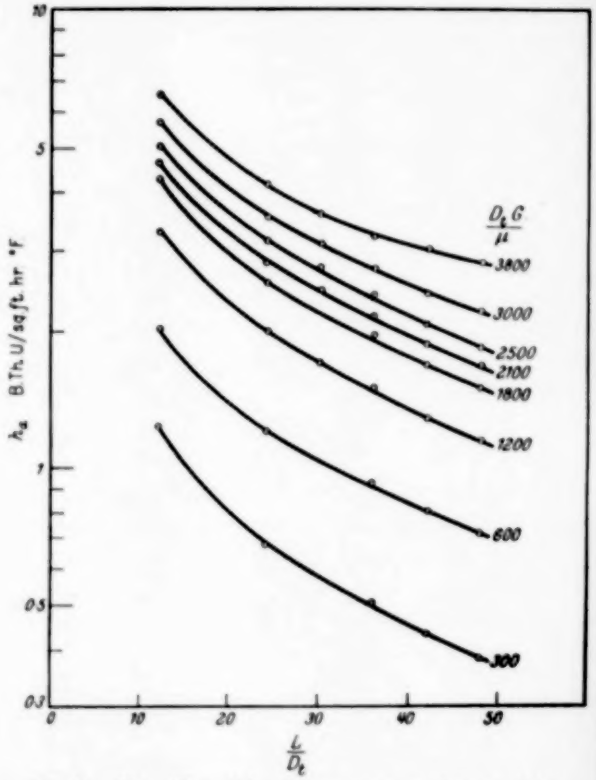

Fig. 14. The effect of length on mean surface conductances.

from a tube of $L/D_t = 42$. The latter values are those based on arithmetic mean temperature difference given in Cholette's Table 4. The curve for $L/D_t = 42$ crosses Cholette's curve at about $Re = 375$, which corresponds to the divergence between the two sets of data at $Gr = 5$–6. The two curves in Fig. 13 are similar in having a minimum at about $Re = 3000$.

The variation in surface conductance with length of heating surface is shown in Fig. 14. These data may be compared with Cholette's Fig. 4 for local coefficients h_x. The coefficients h_x were measured for a short length of tube about the stated L/D_t position from the tube entrance. The average conductances reported here will continue to fall when h_x has attained a constant value with increasing tube length.

between the curve CC and that obtained from an earlier but similar apparatus (Fig. 1) shown as DD on Fig. 12. This apparatus had $D = 1{\cdot}22$ in. and $L = 9{\cdot}56$ in. Curve DD changes gradient abruptly at about $Gr = 25$ to a value of 0·4 and then increases therefrom above $Gr = 140$–150. This increase corresponds to the transition region at $Re > 0200$ for $L/D_t = 7{\cdot}84$. The Cholette data were all for $Re < 2200$, and hence do not show this increased gradient. The present results for the curve CC appear to omit the 0·4 gradient region and show a transition region gradient of 0·7 for $Gr > 5$–6, probably leading to a slightly higher gradient for the turbulent region. Had the data confirmed the Cholette or curve DD pattern they would have shown a change to gradient 0·4 at $Gr = 5$–6, followed by lines breaking away to a gradient near 0·7 at about $Re = 2000$ for each

tube length. The present tubes of L/D_t from 12 to 48 would show breaks at about Gr from 96 to 24 respectively. No indication of this form can be seen in curve CC on Fig. 4, showing that the inlet disturbance has eliminated the 0·4 gradient region and extended the higher gradient transition region from $Gr = 5$–6 upwards. That the curves will change gradient slightly from 0·7 near the upper limits for the Graetz group mentioned above is more obvious from the plot in Fig. 9.

The difference between curves CC, DD is marked, but not readily explained. The curve DD is for a shorter tube than those appropriate to the CC data, but the inlet and outlet conditions to the tube were the same in both series of tests. The only observed difference between the DD and CC tubes was that the DD tube was a smooth surface drawn tube, made up with an expanding jacket and all joints with rubber bungs. The CC tube was heated a number of times during the fabrication of the unit and was cleaned with emery paper before use. The tube surface was considerably rougher than that of the DD tube, and this may have been the major cause of the discrepancy between the two curves in Fig. 12.

The data CC for the tube $D_t = 1$ in. are similar in form to those given as AA from the tube $D = 1{\cdot}22$ in. using the inlet section "a" (Fig. 2) and outlet section "a" (Fig. 3). The outlet condition in the latter case was likely to cause thermometric error due to the radiation from the hot wall. The probable error has been calculated and gives the change from AA to data BB in Fig. 12. The change from BB to CC is thus probably due to the flow changes induced by replacing the end sections "a" by the sections "e".

The curve DD for the tube $D_t = 1{\cdot}22$ in., $L = 9{\cdot}6$ in. is the only one tending towards the accepted correlation for turbulent motion as given by the equation

$$\frac{h D_t}{k} = 0{\cdot}023\,(Re)^{0{\cdot}8}\left(\frac{c\mu}{k}\right)^{0{\cdot}4}. \qquad (10)$$

This equation is for surface conductances based on the logarithmic mean of the terminal temperature differences but the difference from h_1 should be within 5% for all the present data. The lines of gradient 0·8 on Fig. 12 show the positions appropriate to eq. (10) for various L/D_t ratios, the lines being extended down to $Re = 2000$, though they are not expected to be accurate at such low levels of turbulence. The equation approximates to the data to be expected for fully developed flow since it was obtained for long tubes. The data CC are for all tube lengths tested and indicate that the disturbed inlet conditions have little effect on the longer lengths but increase the surface conductances for the shorter lengths in the flow range tested.

Nomenclature

c = specific heat of air at constant pressure; B.Th.U./lb °F

D_t = diameter of tube; ft (unless stated otherwise)

D_p = diameter of packing; ft (unless stated otherwise)

G = flow rate; lb/hr sq ft, (based on tube cross-sectional area)

h = surface conductance; B.Th.U./sq ft hr °F; h based on logarithmic mean of terminal temperature differences, h_a based on arithmetic mean of terminal temperature differences, h_x local surface conductance

k = thermal conductivity of air; B.Th.U.ft/sq ft hr °F

L = length of heated surface; ft

W = flow rate; lb/hr

μ = viscosity of air; lb/ft hr

$Gr = \left(\frac{Wc}{kL}\right)$, dimensionless

$Nu = \left(\frac{h_a D_t}{k}\right)$, dimensionless

$Re = \left(\frac{D_t G}{\mu}\right)$, dimensionless

References

[1] Agarwal, O. P. and Storrow, J. A.; Chem. Ind. 1951 (April) 321. [2] Boussinesq, J.; Comptes Rendus 1891 **113** 9, 49. [3] Cholette, A.; Chem. Eng. Prog. 1948 **44** 81. [4] Chu, Y.C.; M.Sc. Tech. *Thesis*, Manchester 1949. [5] Chu, Y.C. and Storrow, J.A.; Heat Transfer to Air Flowing through Packed Tubes. *This Journal*. 1952 **1** 230. [6] Dryden, H. L.; Quart. Appl. Math. 1943 **1** 7. [7] Goldstein, S.; Modern Developments in Fluid Dynamics, p. 224–9, 233. Oxford University Press, 1938. [8] Leva, M.; Ind. Eng. Chem. 1947 **39** 857. [9] McAdams, W. H.; Heat Transmission, p. 188, McGraw Hill Book Co., New York 1942. [10] Prandtl, L. and Tietjens, O. G.; Applied Hydro- and Aerodynamics, pg. 22–25, McGraw Hill Book Co., New York 1934. [11] Schiller, L.; Z. angew. Math. Mech. 1922 **2** 96. [12] Whitwell, J. C.; Ind. Eng. Chem. 1938 **30** 1157.

Heat transfer to air flowing through packed tubes

Y. C. Chu and J. Anderson Storrow

(Received 6. December 1951)

Summary—A study has been made of the transfer of heat from a heated wall to air flowing through packed beds in a tube of 1 in. diameter. The data are correlated by equations:

(a) for $\frac{D_t G}{\mu} < 1600$; $G < 900$:

$$\frac{h D_t}{k} = 0{\cdot}134 \left(\frac{D_p}{D_t}\right)^{-1{\cdot}13} \left(\frac{L}{D_t}\right)^{-0{\cdot}90} \left(\frac{D_p G}{\mu}\right)^{1{\cdot}17}$$

(b) for $1600 < \frac{D_t G}{\mu} < 3500$:

$$\frac{h D_t}{k} = 15 \left(\frac{L}{D_t}\right)^{-1{\cdot}82} \left(\frac{D_p}{D_t}\right)^{-0{\cdot}90} \left(\frac{D_p G}{\mu}\right)^{m}$$

$$m = 0{\cdot}55 \left(\frac{L}{D_t}\right)^{0{\cdot}165}.$$

The thermal conductivity of the packing has no influence in region (a) but affects the transfer in region (b). The flow rates used were lower than those reported by Leva *et alii* ([1], [2], [3]), but it appears likely that the present data trend to agreement with the functions proposed by Leva as the flow rate is increased.

The most significant features of these results are that in the flow ranges studied the length of the packed tube is an important variable, but the packing diameter has little effect on the heat transfer.

Résumé—Etude expérimentale de la transmission de la chaleur entre la paroi chaude et l'air qui parcourt un tube à garnissage de 25 mm de diamètre. Les équations ci-dessus (a et b) représentent les résultats expérimentaux.

La conductibilité du garnissage est sans influence dans le régime a, mais affecte la transmission dans le régime b. Les débits utilisés sont plus faibles que ceux de Leva *et coll.* [1], [2], [3]. Il semble bien que les résultats actuels tendent vers les formules proposées par Leva, quand les débits croissent.

Conclusion la plus significative à tirer des mesures: dans la gamme des débits étudiés, la longueur du tube garni est une variable importante, tandis que le diamètre du garnissage n'a qu'un faible effet sur la chaleur transmise.

VOL. 1 1952

As part of the study of heat transfer in packed bed catalyst tubes, tests were made of the heat transfer from a heated tube wall to gas flowing through packing within the tube (Chu [4]). The primary object of these tests was to assess the effect of packing diameter to tube diameter ratio, packing length to tube diameter ratio and the effect of thermal conductivity of the packing material, as previous publications did not consider these factors (Colburn [5], Leva [1]). Owing to the limited apparatus available the flow rates were restricted to below 2000 lb/sq ft hr based on the empty tube cross-sectional area. The packings available gave a 50:1 range of thermal conductivity. The L/D_t ratio was varied over a 4:1 range. During the course of this work Leva *et alii* ([2], [3]) published data from similar studies. Their ranges of flow rate were mainly higher than those reported below, and it is considered that the present data are complementary to those of Leva. This consideration has been included with the discussion of the results.

Experimental Technique

The apparatus used is shown in Fig. 1 incorporating the inlet and outlet sections found most suitable after trials of various designs to minimise the errors in measurement of terminal temperatures for the air stream. The coned inlet section reduced the distortion of flow distribution to the packing and provided insulation to reduce heat transfer to the air from the inlet tube below the flange. The cork insulation at the outlet was drilled as shown to exclude radiation from the packed bed to the thermometer measuring the gas temperature. The 1 in. bore copper tube and the 2½ in. bore jacket were reduced in stages from the length shown in Fig. 1 to give heated lengths of 48, 42, 36, 30, 24, 12 in. After each reduction in length the connections to the inner tube and the dimensions of the outlet head were re-made to those in Fig. 1. In each case the copper tube was filled with packing to the level of the top of the steam jacket, the effective length L quoted below being the steam-heated length. The cork inserts at the inlet and outlet reduced the error produced by heat transfer from the tube walls outside the nominal heating length. The packings used were all either spherical or nearly so, and of smooth surface. The *Socony-Vacuum* ("Sova") catalyst beads were not uniform in size. The mean diameter of a large number was 0·145 in. The glass beads were sufficiently

near uniformity to consider them of constant diameter and packings were used with $D_p = 0{\cdot}191$ and 0·0388 in. The lead shot were uniform in diameter and packings were used of $D_p = 0{\cdot}255$, 0·182, 0·126, 0·0951, 0·0426 in. Polished steel balls of diameter 0·250 in. were also used.

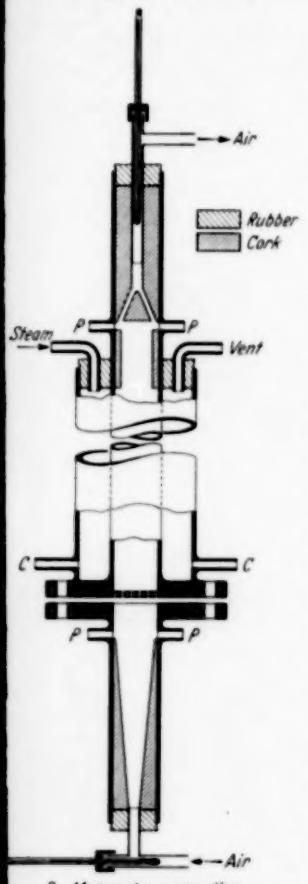

Fig. 1. Heat transfer apparatus.

The packing was supported on a perforated plate drilled with $\frac{1}{8}$ in. dia. holes spaced $\frac{1}{16}$ in. apart. A disc of 60 mesh gauze was placed between the packing and the perforated plate.

The air to the heated tube was supplied through capillary flowmeters calibrated by the plotting technique of Whitwell [6]. The flow was smoothed sufficiently to reduce pressure fluctuations at the inlet to the bed to within 1 mm in 700 mm water gauge pressure difference across the packed bed. The temperature and pressure of the air were measured at stages through the meters and supply tubes for estimation of the mass flow rate and frictional energy loss in the bed. Steam temperatures were measured with thermometers at the inlet and condensate outlet to the steam jacket, since sufficient excess steam was used to blow through the vents to remove rapidly noncondensible gases and condensate, and the pressure in the steam space was greater than atmospheric.

The temperatures of the air stream at inlet and outlet to the packed bed were measured with thermometers graduated to 0·1° C and appropriately calibrated. Even in this small apparatus tests had to be made for times up to an hour at the low air rates for steady state conditions to be attained.

Experimental Results

Tests were made for various air rates covering the range available from the existing equipment in the laboratory. The series of packings were used for tests of different tube lengths to assess the effect of the ratios of tube diameter to packing diameter and of the tube length to tube diameter. The results of these tests are

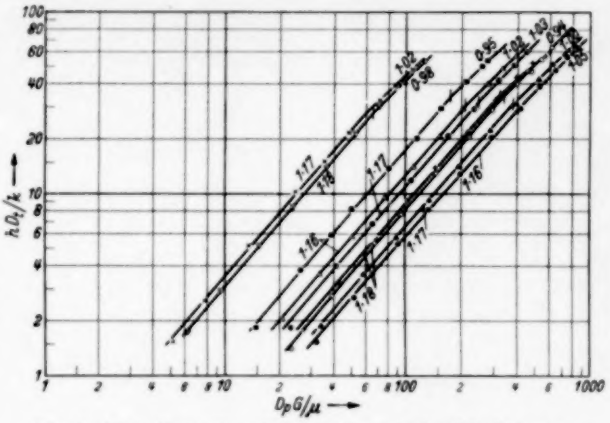

Fig. 2. The effect of packing on the relationship between Nusselt number $\frac{h\,D_t}{k}$ and Reynolds number $\frac{D_p G}{\mu}$.

Packing length = 30 in. = L
tube diameter = 1 in. = D_t

Packing	*Symbol*	D_p *in.*	*Run*
lead shot	●	0·255	56
	○	0·182	57
	△	0·126	58
	■	0·095	59
	▽	0·0426	60
glass spheres	+	0·191	54
	×	0·0388	61
steel balls	▲	0·250	55
sova beads	◐	0·145	62

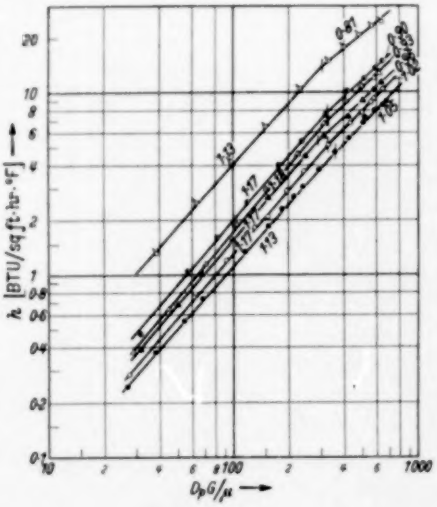

Fig. 3.

L/D_t	*Symbol*	*Run*	L/D_t	*Symbol*	*Run*
48	●	43	30	△	54
42	○	47	24	◐	64
36	▲	51	12	◌	68

Glass spheres $D_p = 0{\cdot}91$ in.

exemplified in Fig. 2, 3, 4, 5. The data in Fig. 2 show the effect of various packing diameters using a fixed tube length, while those in Fig. 3, 4, 5 are for one packing and various lengths of bed. The surface conductances reported for transfer in packed beds were based on the mass flow rate and mean temperature changes of the air stream, the tube inner surface, and the logarithmic mean of the terminal temperature differences between the steam and air streams. The thermal

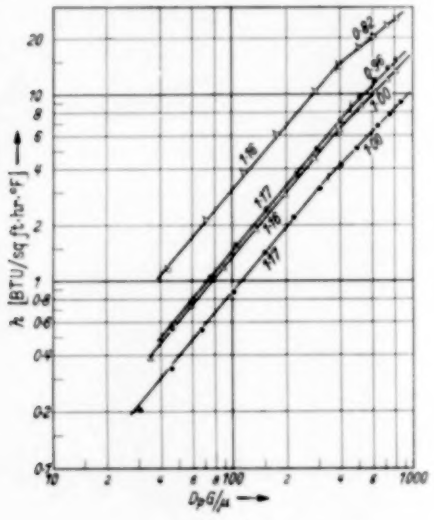

Fig. 4.

L/D_t	Symbol	Run
48	○	45
30	△	55
24	◐	65
12	○	69

Steel balls $Dp = 0{\cdot}250$ in.

resistances for the steam side and the copper tube wall were negligible in comparison with that of the air stream and the temperature of the inner face of the copper tube could be taken as that of the steam without appreciable error. The values of the physical properties of the gas used in graphs and correlations were assessed for the mean temperature of the air in the packed bed.

The data all show lines of the same gradient for flow conditions below a specific Reynolds Number, $\frac{D_p G}{\mu}$, for each packing and tube length. The critical value of $\frac{D_p G}{\mu}$ is affected by packing dimension (Fig. 2) but is almost independent of packed length (Fig. 3, 4, 5). As this breakpoint was to be used as a limit dividing two possible correlation regions of the present data, it was of value either to define its variation or to express it in constant terms. It was found that the variation in the critical Reynolds Number, $\frac{D_p G}{\mu}$, of 56–400 in Fig. 2, 285–350 in Fig. 3, 340–460 in Fig. 4, 390–450 in Fig. 5 was reduced considerably by using the analogous expression for the tube diameter. The groups above gave mean values for $\frac{D_t G}{\mu}$ of 1660 for the Fig. 2, 3, 1560 for Fig. 4 and 1610 for Fig. 5, most of the values lying

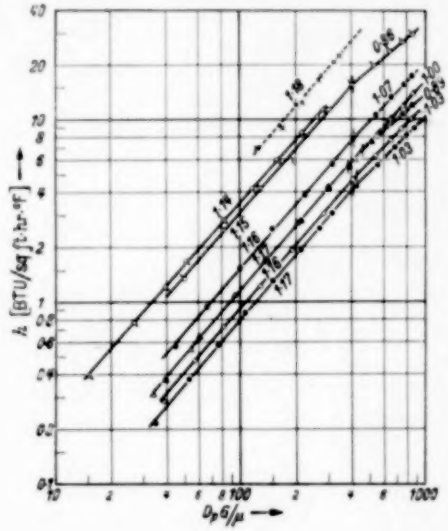

Fig. 5.

L/D_t	Symbol	Run	D_p/D_t	L/D_t	Symbol	Run	D_p/D_t
48	●	44	0·255	24	◐	66	0·255
42	○	49	0·255	12	○	70	0·255
36	▲	52	0·255	30	○	59	0·095
30	△	56	0·255	17	×	Leva	0·1104

Lead shot

Fig. 3, 4 and 5. The effect of length of heat transfer surface on the variation of surface conductance with flow rate.

well within ±10% of the mean. A value of 1600 was accepted for all packings and tube lengths as a critical value of $\frac{D_t G}{\mu}$ being the upper limit of the correlation region at low flow rates.

Correlation for $\frac{D_t G}{\mu} < 1600$

The data in Fig. 2, 3, 4, 5 show a common relationship

$$\frac{h D_t}{k} = \alpha \left(\frac{D_p G}{\mu} \right)^{1{\cdot}17} \qquad (1)$$

where α is probably a function of D_p/D_t and of L/D_t. The data for $L = 30$ in. in Fig. 6 agree with the function

$$\alpha = \beta \left(\frac{D_p}{D_t} \right)^{-1{\cdot}13} \qquad (2)$$

VOL. 1 1952

and the data for the other lengths have similar functions with β as a probable function of L/D_t.

The value β is shown in Fig. 6a, to conform to

$$\beta = \gamma \left(\frac{L}{D_t} \right)^{-0.90} . \qquad (3)$$

The value of γ is independent of the other packing characteristics, particularly thermal conductivity, the data for all packings and tube lengths tested for $\frac{D_t G}{\mu} < 1600$ being in close agreement with the equation

$$\frac{h D_t}{k} = 0.134 \left(\frac{D_p}{D_t} \right)^{-1.13} \left(\frac{L}{D_t} \right)^{-0.9} \left(\frac{D_p G}{\mu} \right)^{1.17} \qquad (4)$$

which has thus correlated data for the ranges; D_p/D_t from 0·0388 to 0·255 and L/D_t from 12 to 48 based on

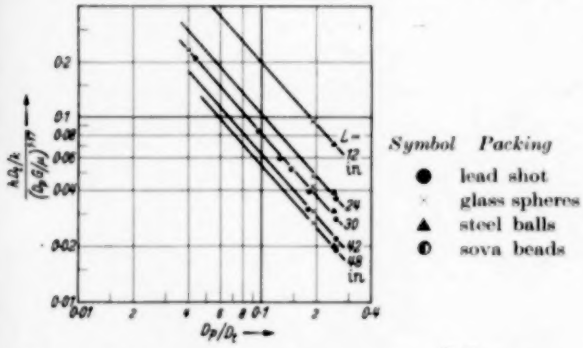

Fig. 6. The effect of packing diameter when $\frac{D_t G}{\mu} < 1600$.

the 1 in. bore tube. It will be noted that in the derivation of eq. (4), as with eq. (8), the dimension D_t has been introduced in the conventional ratios D_p/D_t and L/D_t but has not been tested as an independent variable. The work of Leva *et alii* ([1], [2], [3]) suggests that correlations of the forms used here will cover the effect of D_t.

Correlation for $1600 < \frac{D_t G}{\mu} < 3500$

Unfortunately the equipment available limited the air flow rate to that corresponding to $\frac{D_t G}{\mu} = 3500$, but the range of data appears to be sufficient to justify the following correlation.

For $\frac{D_t G}{\mu} > 1600$, *i.e.* above the break point on each line in Fig. 2, 3, 4, 5 the gradient of the plots decreases below 1·17. On Fig. 2 it seems that this lower gradient remains almost constant for various particle sizes at constant L/D_t ratio, though on Fig. 3, 4, 5 the gradients vary considerably for different L/D_t ratios. With the limited data available (Table 1) the gradient may be assumed dependent only on the length of the packed beds. The plot in Fig. 7 shows the straight line drawn through the values for glass beads, and this line is in reasonable agreement with the data for the other

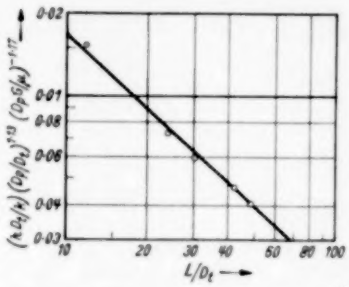

Fig. 6a. The effect of heating length when $\frac{D_t G}{\mu} < 1600$.

materials. The lines on Fig. 2, 3, 4, 5, thus suggest the form

$$\frac{h D_t}{k} = K_1 \cdot \left(\frac{D_p G}{\mu} \right)^m . \qquad (5)$$

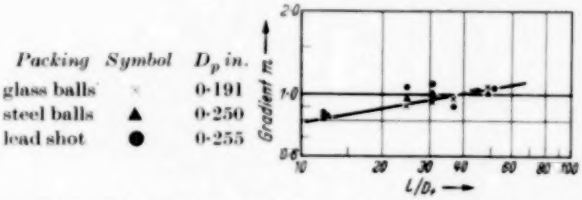

Fig. 7. The effect of heating length on the function of $\frac{D_p G}{\mu}$ when $1600 < \frac{D_t G}{\mu} < 3500$.

Table 1. Values of gradient m. Data from Fig. 3, 4, 5

L/D_t	*Glass beads* $D_p = 0.191$ *in.*	*Steel balls* $D_p = 0.250$ *in.*	*Lead shot* $D_p = 0.255$ *in.*
48	1·05	1·00	1·03
42	1·02	—	1·03
36	0·96	—	0·89
30	0·93	1·00	1·09
24	0·90	0·96	1·07
12	0·81	0·82	0·82

Data from Fig. 2
All packing materials. $L/D_t = 30$

D_p/D_t	*Gradient m*
0·255	1·05
0·250	1·00
0·191	0·94
0·182	1·02
0·145	1·03
0·126	1·02
0·095	0·95
0·0426	0·99
0·0388	1·02

From Fig. 7,

$$m = 0{\cdot}55\left(\frac{L}{D_t}\right)^{0{\cdot}165}. \tag{6}$$

The data from Fig. 2 have been analysed to find the value K_1 in eq. (5) using the power m from eq. (6).

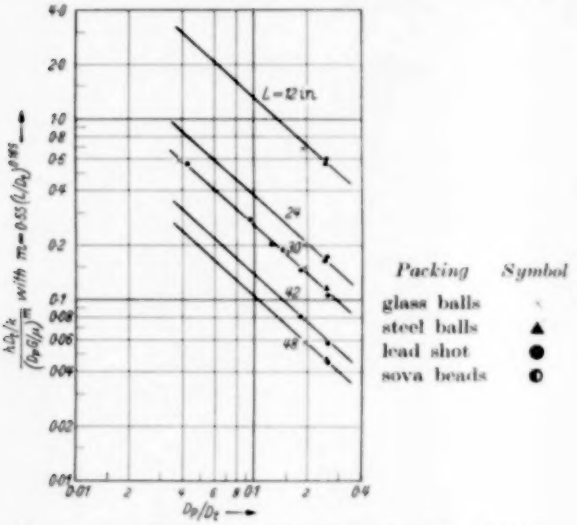

Fig. 8. The effect of packing dimension when $1600 < \frac{D_t G}{\mu} < 3500$.

The plot in Fig. 8 shows a straight line for $L/D_t = 30$ of gradient $-0{\cdot}90$. Similar lines would probably describe the variations of K_1 with D_p/D_t for other L/D_t ratios.

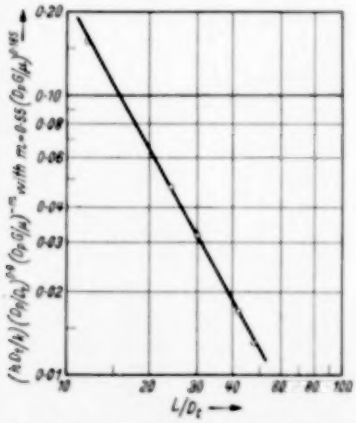

Fig. 9. The effect of heating length when $1600 < \frac{D_t G}{\mu} < 3500$.

Thus accepting

$$K_1 = K_2\left(\frac{D_p}{D_t}\right)^{-0{\cdot}90} \tag{7}$$

is shown that the effect of thermal conductivity is K_2 is probably a function of L/D_t. The data shown in Fig. 9 are the mean values of K_2 for the values at each L/D_t ratio. They conform to a straight line of gradient $-1{\cdot}82$. The data for air flowing through various materials, packings and packed lengths are all correlated for $1600 < \frac{D_t G}{\mu} < 3500$ by the eq. (8), (8a):

$$\frac{h D_t}{k} = 15\left(\frac{L}{D_t}\right)^{-1{\cdot}82}\left(\frac{D_p}{D_t}\right)^{-0{\cdot}90}\left(\frac{D_p G}{\mu}\right)^{m} \tag{8}$$

$$m = 0{\cdot}55\left(\frac{L}{D_t}\right)^{0{\cdot}165}. \tag{8a}$$

A function of Prandtl Number $\left(\frac{c\mu}{k}\right)$ has not been included in the correlation equations. In view of the probability that the appropriate function varies less than 2% for the experimental range, such an inclusion cannot be assessed from the present data.

Discussion of Results

It had been expected that the thermal conductivity of the packing would influence the heat transfer, and

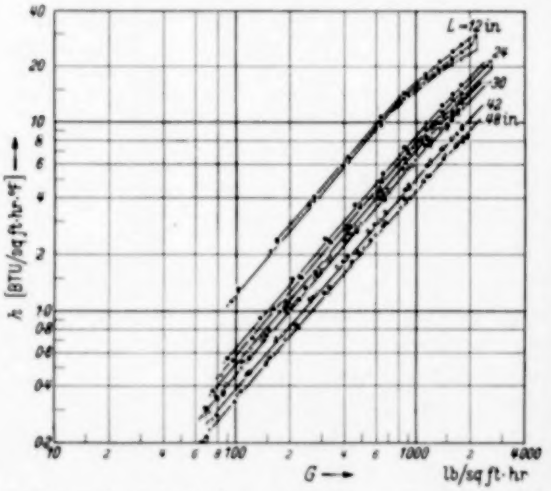

Packing	Symbol	D_p in.	Packing	Symbol	D_p in.
lead shot	●	0·255	glass balls	+	0·191
	○	0·182		×	0·0388
	△	0·126	steel balls	▲	0·250
	■	0·095	sova beads	◐	0·145
	▽	0·0426			

Fig. 10. The effect of flow rate on surface conductance for various packings and heating lengths.

during this work a publication by Leva and Grummer [2] discussed results showing that the transfer coefficients for a similar system increased with thermal conductivity of the packing material. In Fig. 10 it insignificant below the break point at $\frac{D_t G}{\mu} = 1600$, approximately at $G = 900$ lb/hr sq ft, though the effect seems to become apparent at higher flow rates. The data of Leva and Grummer [2] were obtained

VOL. 1 1952

at higher flow rates except for their tests on lead shot and aloxite particles. These tests are referred to later as the present data explain what Leva considered to be anomalous results for lead shot. Considering the lengths $L = 48$ in. and $L = 42$ in. in Fig. 10, the points for lead shot $D_p = 0{\cdot}255$ in., steel balls $D_p = 0{\cdot}250$ in., and glass beads $D_p = 0{\cdot}191$ in. all lie on one line for a given packed length. For other lengths of packed beds the data for packing of greatly differing thermal conductivity also lie near the same line. The effect of D_p differences should be taken into account in this comparison but from eq. (4) it is seen that the effect of D_p on h is small since $h \propto D_p^{0{\cdot}01}$. Thus a ten-fold change in D_p alters h by 10%, and the maximum ratio of two particle sizes in the present tests was only 6·6. The small effect of particle size in this range is demonstrated by the data in Fig. 10.

Above the limit near $G = 900$, $\frac{D_t G}{\mu} = 1600$, the extent of the present data is sufficient to suggest that thermal conductivity of the packing begins to affect h. In Fig. 10 the data for $L = 24$ in. and $L = 12$ in. show that at the highest flow rates, the lines for glass beads are falling away from those for lead shot and steel balls. This trend is also obvious from the gradients shown in Table 1. The present data thus appear to lead towards the results of Leva and Grummer showing the effect of thermal conductivity in the higher flow ranges of $G = 500$ to 4000.

Leva and Grummer [2] found h proportional to the 0·8 to 0·9 power of $\frac{D_p G}{\mu}$ except for their data on lead shot which have been included in Fig. 5. The Leva results were not anomalous, conforming to the lower flow rate region in the present work, probably being below the break point corresponding to those shown on Fig. 5, whilst the rest of Leva's results were obtained for the higher flow region where the power 0·8–0·9 would be expected from the present data. The existence of the region of high gradient 1·17 does not appear to have been recognised elsewhere in the case of fixed beds except by Schumacher [7]. The present data confirm work on the fine powder packings (Agarwal and Storrow [8]) whether static or fluidized. The Leva [1] data for glass beads $D_p = 0{\cdot}172$, $D_t = 2{\cdot}0$ in. also show the trend to a higher power than 0·8 with decreasing flow rate. The data of Leva, Weintraub and Grummer [9] for fluidized beds appear to confirm the high gradient above. Their results show $h \propto G^{1{\cdot}15}$, and it has been shown (Agarwal and Storrow [8]) that the appropriate plots of data for fluidized beds continue the curves for the associated packed bed at lower flow rates, and show the same dependence on mass velocity. The Leva power 1·15 is thus a possible confirmation of the present power 1·17. There is a difference which must be noted in that the Leva, Weintraub and Grummer surface conductances were obtained from the integrated mean temperature difference based on a temperature survey along the flow path of the gas, whereas the present data are based on the logarithmic mean of the terminal temperature differences.

The equations obtained above have been checked against the data used in their construction and it was found that the eq. (4) agreed with all experimental results to less than ±10% and with the majority of results to less than ±5%. A comparison has also been made with the few data from Leva's tests which are in the same flow region, *i.e.* (a) those for glass beads $D_p = 0{\cdot}172$ in. in a tube of $D_t = 1{\cdot}96$ and $L = 36$ in., and $D_p = 0{\cdot}388$ in. in the same tube, from Leva [1], (b) those for lead shot of $D_p = 0{\cdot}091$ in. in a tube of $L = 14$ in. and $D_t = 0{\cdot}824$ in. In these cases the eq. (4) gave h values 19·9 to 22·3% higher than the observed values. On checking data for an earlier apparatus for thermometer arrangements similar to those employed by Leva it was found that they were about 14% higher than the eq. (4) values. The data referred to were considered unsatisfactory primarily owing to the radiation errors to the thermometers concerned. The data of Leva [1] and Leva and Grummer [2] may be in error by a similar amount. This may have contributed to the fact that on reversing the direction of heat transfer in their apparatus Leva, Weintraub, Grummer and Clark [3] found surface conductances for cooling the gas about 15% higher than those from the Leva correlations of conductances when heating the gas.

Another difference between the present results and those of Leva lies in the function of the ratio D_p/D_t adopted. Leva [1] used the exponential function $\epsilon^{-6 D_p/D_t}$ to cover the wall effect dependent on D_p/D_t. The data for the higher ranges of flow tested by Leva, for which the appropriate power of Reynolds Number was 0·9, agreed with a straight line when plotted as

$$\log \frac{h D_t}{k} \Big/ \left(\frac{D_p G}{\mu}\right)^{0{\cdot}9}$$

against D_p/D_t as in Fig. 5 of Leva [1]. The data for a similar range of D_p/D_t to that for the present results

could be approximated by a function

$$\frac{h\,D_t}{k} \Big/ \left(\frac{D_p G}{\mu}\right)^{0.9} \propto \left(\frac{D_p}{D_t}\right)^{1.1}$$

similar to that used here, though the agreement between the experimental points and this form is less

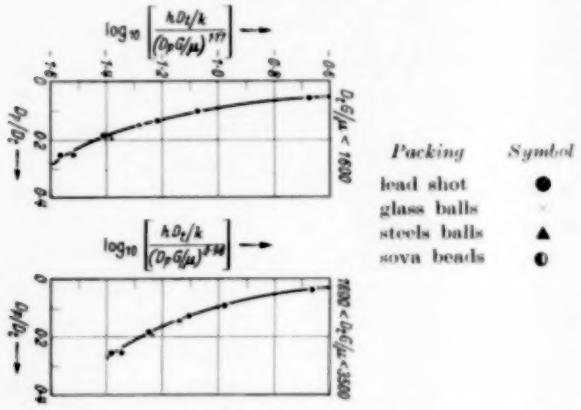

Fig. 11. The failure of the exponential function for the effect of D_p/D_t.

than with the exponential form above. The exponential form may be correct for the higher flow rates but for the two regions in the present work, the form is unsatisfactory for correlation purposes as shown in Fig. 11. Using the ordinate appropriate to each flow region the curvature of the plots is pronounced, though it should be noted that the data in Fig. 5 of Leva [1] show similar curvature, though less pronounced. The simple power functions of D_p/D_t used in eq. (4), (8) will not show a maximum in a plot of $h/G^{1.17}$ or h/G^{m} respectively against D_p/D_t. The exponential function of D_p/D_t used by Leva does show this maximum at $D_p/D_t = 0{\cdot}15$ in agreement with the experimental data at the higher flow rates. Leva, Weintraub, Grummer and Clark [3] discuss the use of these D_p/D_t functions.

Conclusions

From consideration of the present data together with those of Leva it appears likely that the heat transfer to gas flowing through packed beds may be covered by the three types of curves shown in Fig. 12. These types cover the probable effects of length of packed bed, the diameter of packing particle and the thermal conductivity of the packing material.

The curves expressing the heat transfer to air flowing through packed tubes having the same ratio D/L_t and different ratios D_p/D_t are of the form in Fig. 12a. The regions ab and bcd are exemplified by the data given in Fig. 2 for five sizes of lead shot for $D/L_t = 30$. The ordinates used in Fig. 2 move the relative positions of the lines but do not alter the forms from those to be expected on plotting h instead of $\frac{h\,D_t}{k}$. The lines for different D_p/D_t ratios in Fig. 12a are parallel to each other in each of the regions ab, bcd.

The curves for heat transfer when the D_p/D_t ratio is constant and L/D_t is varied are exemplified by Fig. 12b, similar to the data in Fig. 3, 4, 5. At $\frac{D_p G}{\mu}$ above the critical point, the lines in bc vary in gradient. This gradient increases with increasing L/D_t ratio. It is reasonable to expect that the lines will converge to give a common line cd. In this flow range cd as covered by Leva's data the surface conductance is independent of L/D_t. Leva, Grummer, Weintraub and Clark tested ratios $L/D_t = 10$ and 17 with $\frac{D_p G}{\mu} = 640$–1400 and found no length effect in the

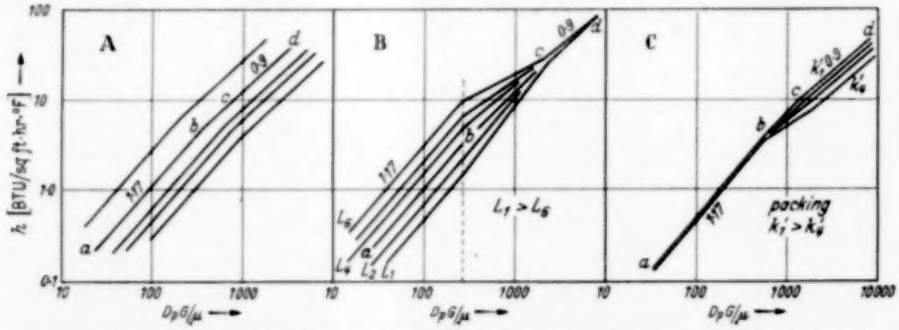

Same packing material. Constant L/D_t, Various D_p/D_t

Same packing material. Various L/D_t, Constant D_p/D_t

Different packing material. Constant L/D_t, Constant D_p/D_t

Fig. 12. The suggested ranges of effect of L, D_p/D_t, and thermal conductivity of the packing.

cooling of gases flowing through packed beds. These data may not have extended down to the region *cd* in Fig. 12b but the present data show that such L/D_t changes under these flow rates would have small effect on the heat transfer equipment.

The vertical broken line in Fig. 12b cutting the lines indicates the critical flow condition ($G = 900$ lb/sq ft hr; $\frac{D_t G}{\mu} = 1600$ for $D_t = 1$ in.) which depends on the ratio D_p/D_t but not on L/D_t.

In Fig. 12c the surface conductances are for packed tubes having the same L/D_t and D_p/D_t ratios but packings of different thermal conductivities. The thermal conductivity has negligible influence in the region *ab* but affects the heat transfer in the region *bc*, leading to the effects measured by Leva and Grummer [2] at higher flow rates, *cd*.

The small effect of D_p leads to a reasonable correlation of all data on a logarithmic plot of $\frac{h D_t}{k}$ against $\frac{D_t G}{\mu}$, agreeing with the observations of Schumacher [6]. This author commented that packings of various thermal conductivities and diameters had little effect on the heat transfer between the retaining wall and the gas flowing through the packing. He found that below a critical Nusselt number, $\frac{h D_t}{k} = 225$, this group was proportional to $\left(\frac{D_p G}{\mu}\right)^{1.0}$, and above this critical value $\frac{h D_t}{k} \propto \left(\frac{D_p G}{\mu}\right)^{0.75}$. Below a critical Nusselt number $\frac{h D_t}{k} = 57$, the form $\frac{h D_t}{k} \propto \left(\frac{D_p G}{\mu}\right)^{1.2}$ was found. Schumacher considers that the Leva correlations based on $\left(\frac{D_p G}{\mu}\right)^{0.9}$ are only valid in the region $57 < \frac{h D_t}{k} < 225$. The present data are for the low flow ranges equivalent to the two lower regions of Schumacher. The data in Fig. 2 show an apparent critical value of $\frac{h D_t}{k}$ at about 30, rather than 57. The gradients below and above their critical value agree with Schumacher's opinion. The lower critical Nusselt number corresponds to the lower critical value of $\frac{D_t G}{\mu} = 1600$ found here as compared to the value 2300 found by Schumacher. Schumacher comments on the necessity for altering Reynolds number by a factor of 2 in the data of Kling [10] to make them agree with those of Leva, mentioning the 3:1 length ratio though D_t and D_p were the same. The present analysis of the length effect explains the origin of such differences.

Note added in proof—Papers in which heat transfer to fluids in packed beds has been analysed in terms of effective thermal conductivity and in which attempts have been made to segregate the thermal resistances in the system are intentionally omitted. These analyses, as exemplified by References [11]–[18], are based on various suppositions which are not correct. The present report is limited to a presentation of data in the form of surface conductances correlated by the usual arguments, rather than discussing the postulated mechanism of the heat transfer. The functions shown prove simpler than one might imagine in view of the probable complexity of the transfer system. It is not expected that the correlation equations for $Re < 1600$ can be extrapolated below the experimental range. The values quoted are already lower than the constant value to be expected at low flow rates. The suggestion that the failure to attain the constant range at higher h values than those shown is due to heat losses from the apparatus [16] seems questionable. The numerical value of the limiting surface conductance and derived Nusselt number depend on the basic definitions of the quantities involved, notably temperature distribution and effective conductivity.

Notation

c = specific heat of air at constant pressure; B.Th.U/lb°F.
D = diameter; D_t for tube; D_p for packing; ft.
G = flow rate based on empty tube; lb/sq ft hr.
h = surface conductance; B.Th.U/sq ft hr°F.
k = thermal conductivity of air; B.Th.U ft/sq ft hr°F.
L = length of heated surface; ft.
μ = viscosity of air; lb/ft hr.

References

[1] Leva, M.; Ind. Eng. Chem. 1947 **39** 857. [2] Leva, M. and Grummer, M.; Ind. Eng. Chem. 1948 **40** 415. [3] Leva, M., Weintraub, M., Grummer, M. and Clark, E. L.; Ind. Eng. Chem. 1948 **40** 747. [4] Chu, Y. C.; M.Sc. Tech. *Thesis* 1949 (Manchester). [5] Colburn, A. P.; Ind. Eng. Chem. 1931 **23** 910. [6] Whitwell, J. C.; Ind. Eng. Chem. 1938 **30** 1157. [7] Schumacher, R.; Erdöl und Kohle 1949 **5** 189. [8] Agarwal, O. P., and Storrow, J. A.; Chem. Ind. 1951 (April) 321. [9] Leva, M., Weintraub, M., Grummer, M.; Chem. Eng. Prog. 1949 **45** 563. [10] Kling, G.; V.D.I.-Forschung 1938 **9** 82. [11] Brotz, W.; Chem. Ing. Technik 1951 **23** 408. [12] Coberley, C. A. and Marshall, W. R.; Chem. Eng. Prog. 1951 **47** 141. [13] Hougen, J. O.; and Piret, E. L.; Chem. Eng. Prog. 1951 **47** 295. [14] Smith, J. M., Morales, M. and Spinn, C. W.; Ind. Eng. Chem. 1951 **43** 225. [15] Smith, J. M., Bunnell, D. G.; Irvin, H. B. and Olson, R. W.; Ind. Eng. Chem. 1949 **41** 1977. [16] Verschoor, H. and Schutt, G. C. A.; Appl. Sci. Res. 1950 **A 2** 97. [17] Wilhelm, R. H. and Singer, E.; Chem. Eng. Prog. 1950 **46** 343. [18] Wilhelm, R. H. and Bernard, R. A.; Chem. Eng. Prog. 1950 **46** 233.

Erratum: Estimation of the free enthalpy (Gibbs free energy) of formation of organic compounds from group contributions*)

D. W. VAN KREVELEN and H. A. G. CHERMIN

Staatsmijnen in Limburg, Central Laboratory, Geleen, The Netherlands

In this paper a number of numerical errors appeared. In calculations involving thermodynamic properties of compounds containing sulphur, bromine and iodine one is forced to choose the gaseous state as the reference state. The ΔH_f^0-respectively ΔG_f^0-values used in these calculations (see section V of our paper) should consequently refer to the gaseous state of sulphur, bromine and iodine. This has, erroneously, not been done in our paper. All values of the free enthalpy of formation should for that reason be corrected by the free enthalpy of transition due to the transition of the elements from the LEWIS and RANDALL reference state to the gaseous reference state.

We recalculated the group contributions and free enthalpies of formation of sulphur, bromine and iodine containing compounds. The corrected values are given in Tables 13, 14, 16 and 17 below (numbering as in the above mentioned paper). The Figs. 4, 6 and 7 should be changed in accordance with the corrected values.

* Chemical Engineering Science 1951 **1** 66.

Table 13

Group	Group contribution $A + \frac{B}{100} . T$				Highest temperature of lit. value
	300 ⋮ 600 °K		600 ⋮ 1500 °K		
	A	B	A	B	°K
H_2S	−20·552	1·026	−21·366	1·167	1500
—SH	−10·68	1·07	−10·68	1·07	1500
—S—	− 3·32	1·42	− 3·32	1·44	1500
⋛S	− 0·97	0·51	− 0·65	0·44	1500
>SO	−30·19	3·39	−30·19	3·39	1200
>SO_2	−82·58	5·58	−80·69	5·26	1200

Table 14

Group	Group contribution $A + \frac{B}{100} . T$				Highest temperature of lit. value
	300 ⋮ 600 °K		600 ⋮ 1500 °K		
	A	B	A	B	°K
HBr	−12·553	−0·234	−13·010	−0·158	1500
—Br	− 1·62	−0·26	− 1·62	−0·26	1200
HI	− 1·330	−0·225	− 1·718	−0·176	1500
—I	+ 7·80	0	+ 7·80	0	1500

Table 17

Compound	Free enthalpy of formation $A + \frac{B}{100} . T$				a °K	Calculated from values given by
	300 ⋮ 600 °K		600 ⋮ a °K			
	A	B	A	B		
SO_2	− 86·657	+1·735	− 86·657	+1·735	1500	16
SO_3	−109·813	+3·943	−109·813	+3·943	1200	51
COS	− 49·414	−0·245	− 49·269	−0·265	1500	11
CS_2	− 3·301	−0·150	− 3·104	−0·177	1500	11

Table 16

Compound	300 °K		600 °K		900 °K		1200 °K		1500 °K		Calculated from literature
	Calculated kcal/mol	Found kcal/mol	Calculated kcal/mol	Found kcal/mol	Calculated kcal/mol	Found kcal/mol	Calculated kcal/mol	Found kcal/mol	Calculated kcal/mol	Found kcal/mol	
Methylbromide . . .	− 6·0	− 6·3	+ 0·5	+ 0·0	+ 7·6	+ 7·0	+14·8	+14·2			49
Methyltetrabromide .	+ 5·0	+ 6·9	+14·6	+16·6							49
Methylbromoacetylene	+44·4	+44·3	+47·5	+48·0	+51·4	+51·3					63
Vinylbromide	+16·3	+15·4	+20·2	+19·9	+24·4	+24·8	+28·9	+29·9	+33·4	+35·1	38
Acetylene di-iodide. .	+66·9	+66·7	+64·0	+64·7	+61·0	+60·7					63
Vinyliodide	+26·5	+26·6	+31·2	+31·0	+36·1	+35·8	+41·4	+40·7	+46·7	+45·7	38
Ethylmercaptane. . .	− 9·7	− 9·5	+ 7·5	+ 7·5	+25·6	+25·6					6
Dimethylsulphide . .	− 7·2	− 7·0	+10·7	+10·8	+30·1	+29·9					6
Thiophene	+20·7	+20·6	+29·9	+29·9	+40·0	+40·0	+50·2	+50·1	+60·4	+60·4	57
Dimethylsulphoxide .	−28·6	−28·6	− 5·2	− 4·9	+19·6	+19·7	+44·6	+44·3			6
Dimethylsulphone . .	−74·0	−74·0	−43·7	−43·6	−12·9	−12·6	+17·9	+17·9			6

VOL. 1 1952

Book reviews

K. G. DENBIGH: **The Thermodynamics of the Steady State.** Methuen & Co. Ltd., London 1951. VIII + 103 pp. 6s. 6d.

The Second Law of Thermodynamics is one of the most powerful tools of science when applied to equilibrium phenomena and reversible processes; in regard to irreversible processes, however, it can provide us with no more than the qualitative information that the entropy increases. The first attempt to extend thermodynamic methods beyond the equilibrium state was made by Lord KELVIN not long after the formulation of the Second Law itself. KELVIN considered a thermo-electric circuit in its steady state, so that a constant temperature difference was maintained between the junctions, and a steady electric current flowed in the circuit. He assumed that, although irreversible processes were an essential feature of the system, the Second Law could nevertheless be applied to the parts of the system which were reversible, and he was thus able to derive relations between the magnitude of the PELTIER and THOMSON heats, and the temperature coefficient of the thermo-electric E.M.F. KELVIN realized clearly that his treatment involved a new hypothesis in addition to the Second Law, and stressed the need for experimental verification of the resulting conclusions; subsequent data were certainly in reasonable agreement with the new equations.

Later writers applied the THOMSON hypothesis to a number of other problems such as the E.M.F. of a concentration cell, and the process of thermal diffusion (the change in concentration associated with a temperature gradient). Irreversible processes were again characteristic of the systems, and the theory was applied to the steady state. For some of these problems a treatment based on the kinetic theory of gases was already available, and the results obtained by the two methods were in agreement.

The major step towards clarifying the nature of the THOMSON hypothesis was made by ONSAGER in 1931. Chemists had always assumed that in an equilibrium involving several independent chemical reactions, there was detailed balancing of the individual reactions, and this was usually taken to be a consequence of the Second Law. ONSAGER showed that although this was correct for a system involving two independent reactions, there was nothing in the Second Law to prevent equilibrium being maintained by cyclic processes when there were more than two independent reactions. A new hypothesis was required if this possibility were to be excluded, the principle of microscopic reversibility, and ONSAGER was able to show that THOMSON's hypothesis was a consequence of this principle. TOLMAN has expressed this principle as follows: "Under equilibrium conditions any molecular process and the reverse of that process will be taking place on the average at the same rate."

The past few years have witnessed a considerable development of the thermodynamics of irreversible processes, and a wide literature has sprung into being. Much of this literature has been somewhat abstruse and scattered, and the subject has remained in the hands of specialists, and has not penetrated to the ordinary research worker. Dr. DENBIGH has performed an extremely valuable service by making available to the wider scientific public a clear and readable introduction to steady state thermodynamics, and this monograph should go a long way towards dispelling the obscurity which has been associated with the subject. The treatment is elementary, and anyone with a knowledge of classical thermodynamics should have little difficulty in following the arguments.

The monograph consists of 6 chapters. Chapter I contains a brief survey of the historical development. Chapter II discusses the application of the THOMSON hypothesis to thermal-migration phenomena. Chapter III is devoted to a discussion of the ONSAGER theory. ONSAGER regards the processes of diffusion and flow of heat and electricity as being representable in terms of velocities, J_i, which describe the rate at which the processes take place, and "thermodynamic forces," X_i, which cause the processes to take place. He assumes that linear relations, $J_i = \sum_{j=1}^{r} L_{ij} X_j$, exist between the velocities and forces, the L_{ij} being coupling coefficients. The theory bears a formal analogy to that of currents in electrical networks, and the principle of microscopic reversibility yields the symmetrical relation $L_{ij} = L_{ji}$. The X_i must be chosen so that $\frac{1}{T}\sum_{i=1}^{r} J_i X_i$ is equal to the rate of generation of entropy per unit volume. Chapter IV considers the rate of increase of entropy in various natural processes, and Chapter V deals with the application to a number of particular problems, such as thermal migration through a barrier, and thermal diffusion in electrolytic solutions. The final chapter discusses the relationship between the THOMSON hypothesis and the ONSAGER theory. Adequate references are given to original papers for those who wish to pursue the subject more thoroughly.

The book can be heartily recommended to physicists, chemists, engineers and all others who are concerned with the applications of thermodynamics. C. DOMB

BERNARD LEWIS and GUENTHER VON ELBE: **Combustion, Flames and Explosions of Gases.** Academic Press Inc., Publishers, New York 1951. 795 pp. Price $ 14.

This book is intended as a standard work on the physical and chemical principles of the combustion process. Its use is recommended to the student, engineer and research worker. It may be said that the authors have fully attained their aim. When comparing this work with the book of the same title published in 1938 and written by the same authors, it cannot properly be called a second edition, as the contents are entirely new, with the exception of a few minor sections, and the text has been considerably enlarged. This enlargement provides a good idea of the great activity in gas-combustion research and technique during the last ten years.

Though a great many of the problems discussed in this book have not been solved definitely by far, the authors by no means give a dry summing-up of facts. Naturally, a large portion of the text is devoted to the experimental and theoretical work of the authors. However, due attention is also given to important work by others. Those who only want orientation in the field concerned will find in this book a well-founded representation of the most varied phenomena, problems and experimental methods which may be encountered in gas combustion. Those who want to enter more deeply into certain subjects will moreover find an extensive and up-to-date (1951) literature list. For practical workers a fine collection of numerical data is given in the form of tables and graphs.

The arrangement of the text is largely the same as in the previous edition. The first part (about 200 pp.) is devoted to the reaction kinetics of the non-catalytic oxidation reactions H_2, CO, hydrocarbons and some oxygen-containing organic substances are treated successively. In this part considerable attention is also paid to the important phenomenon called "engine knock."

The second part of the book deals with flame propagation (over 400 pp.). Much attention is given to the theory of the

flame front and to ignition. Moreover this part contains discussions of diffusion flames, detonations and turbulence.

The treatment of burners with air entrainment is of great practical importance.

Part III deals with the state of the burned gas (60 pp.), while Part IV (30 pp.) is devoted to the technical application of gas combustion in industry and in engines. This last part is very brief and contains a survey of the basic principles only.

The scope of the work under discussion does not allow of giving an extensive treatment of these subjects; this would require a separate book.

The final 30 pp. are reserved for several valuable tables, containing *e.g.* thermodynamic data on gas reactions, flame temperatures and explosion limits.

The production of the book is excellent. In spite of its price, which according to European standards is perhaps rather high, it should be bought by everyone concerned with the combustion of gases.

Dr. J. VAN STEENIS

Ullmanns Encyclopädie der Technischen Chemie. Dritte völlig neugestaltete Auflage (Editor: Dr. WILHELM FOERST) Band I: Chemischer Apparatebau und Verfahrenstechnik. (Co-Editors: Prof. Dr. E. WICKE and Dipl.-Ing. E. RÖMER). Publishers: Urban & Schwarzenberg, München-Berlin 1951. XXII + 1011 pages, 18,5 × 26,5 cm. DM 108.—

Since the publication of the first edition of ULLMANNS famous handbook it has proved to be one of the great standard works in chemical literature. It is remarkable how even this first attempt was a success in every way; and since then this encyclopaedia has become indispensable for the industrial chemist and the chemical engineer as well as for the metallurgical and mining engineer and workers in other fields of applied science. The last edition was published between 1928 and 1932, so that at the moment the handbook is more than 20 years old. It was reprinted after 1933 without revision, the only difference being that the name of the creator of this work was not allowed to appear on the title page. The work has found a successor in the U.S.: the Encyclopaedia of Chemical Technology, edited by KIRK and OTHMER and published from 1947 on with 13 volumes appearing at 7-month intervals.

Owing to the impetuous development of chemical engineering since 1930, ULLMANNS old Encyclopaedia is now out of date in many respects, and for this reason the appearance of a new edition is very fortuitous.

The first volume of the new edition has now been issued. Whereas the former editions of this handbook were arranged alphabetically according to catchwords, the first two of the new volumes show a different order. Volume I contains a systematic survey of Chemical Engineering in a logical arrangement. Successive chapters deal with thermodynamics and flow of fluids, pressure and vacuum techniques, heating and cooling, separating and mixing processes; and finally a discussion of reactors and another about construction materials are given. Naturally, many experts have contributed to the chapters devoted to their particular fields of study.

Each chapter is preceded by a comprehensive table of contents, printed on thick yellow paper. Besides, two indexes have been inserted at the end of the book, one general and another for the chapter on construction materials. A list of authors is lacking, which is to be regretted. In many places literature references are given, naturally to a limited extent. European literature is given prevalent attention.

Volume I is a beautiful book in a splendid binding, printed on high-quality paper and containing 1400 exceptionally fine figures.

In all respects the first impression the book makes is a favourable one. It is understandable that a work like this has its weeknesses. The treatment of thermodynamics is very brief, as is *e.g.* that of the separation of homogeneous gas mixtures (*i. a.* gas absorption). Presumably every specialist will hit on shortcomings in his own field. After all, with books of this scope the selection of the material to be treated is a matter of taste. Yet every one in possession of this work will find quick orientation possible.

The book contains a number of splendid systematic and tabular surveys, *e.g.* of vacuum pumps, dimensionless heat transfer equations, crushing and grinding plants, etc. ChapterVI gives a complete and comprehensive survey of reaction apparatus, such as is not often met with elsewhere.

To sum up, it should be said that editors and publishers may well be congratulated on the appearance of this book, which may be called indispensable for libraries. It is hoped that the volumes will appear at fairly short intervals and that they will live up to the standard promised by the first. However, the price of works like this is so high that only very few private persons will be able to afford the luxury of buying them.

D. W. VAN KREVELEN

VOL. 1 1952

ERRATA

Chem. Eng. Science Vol. I, No. 4, Hydroextraction—IV by M. M. HARUNI and J. ANDERSON STORROW.

(1) in last six lines (column 2) page 157 and first six lines (column 1) page 158:

substitute "B" for "A"
"C" for "B"
"A" for "C".

(2) equation 9, page 161:

include "μ" in numerator of right hand side: to read "μqg" instead of "qg".